



CHALMERS
UNIVERSITY OF TECHNOLOGY



Effects of Fault Zones and Hydrothermal Alteration on the Physical Properties of Crystalline Rocks

Master's thesis in Innovative Sustainable Energy Engineering (Heat and Power)

WASEEM ULLAH



CHALMERS
UNIVERSITY OF TECHNOLOGY

Department of Space, Earth, and Environment
CHALMERS UNIVERSITY OF TECHNOLOGY, Gothenburg, Sweden, 2025

Effects of Fault Zones and Hydrothermal Alteration on the Physical Properties of Crystalline Rocks.

WASEEM ULLAH

© WASEEM ULLAH, 2025

Department of Space, Earth, and Environment
Chalmers University of Technology
SE-412 96 Göteborg
Sweden

Preface and acknowledgements

I would like to express my appreciation to the whole team involved in this study. I am thankful to Bischof Alan, who provided me with the opportunity to work with the Deep Heat Flows project. I am also thankful for his valuable opinions as an advisor during the whole study. The data used in this study were obtained from the Deep Heat Flows project. Moreover, I appreciate the time and effort put in by Kiuru Risto throughout the analysis and writing process as an advisor. I am also thankful to Tobias Mattisson for supervising this thesis and giving his valuable insights when needed.

Nonetheless, I would like to thank my parents, Habib Ullah, Fatima Habib, siblings, and friends for their unwavering support throughout my academic journey. They were always a source of motivation and courage.

Portions of this thesis were developed with the assistance of artificial intelligence tools, specifically OpenAI's ChatGPT, which was used for language refinement, idea organization, grammar correction. All content was critically reviewed and approved to ensure academic integrity and originality.

Otaniemi, Espoo, Finland, 28 April 2025.

Waseem Ullah

Abstract

Understanding the physical properties of rocks, such as seismic wave velocities, acoustic impedances, density, porosity, and thermal conductivity, is crucial to the exploration and production of geothermal energy. Thermal conductivity in a bore hole can be measured directly, but it takes more time and has less reliability as compared to laboratory (indirect) methods. This study primarily focuses on seismic wave velocities and thermal conductivity, while also considering the variation of other parameters under different rock conditions, namely massive, brecciated, fractured, and altered types with varying porosity values.

The goal of this study was to find an association between these parameters and to determine if such associations can be quantified or not. These studies were carried out in the fault and fracture zones of Finland (with up to 30 % porosity values). The findings from this thesis can contribute to identifying suitable geothermal reservoirs that support efficient heat transfer and fluid storage, emphasizing the importance of optimized porosity values. The physical properties of crystalline fault zone rocks in Southern Finland were already available from laboratory measurements of density, porosity, thermal conductivity, and seismic wave velocities. These physical properties served as input data for statistical analysis tools application including Spearman's rank test, Chi-square tests, and Fisher's exact test in this study. To create predictive equations/models for the parameters being compared, regression analysis was performed using Microsoft Excel to determine whether the associations could be quantified or not.

A clear, significant, positive monotonic relationship was found between seismic wave velocities and thermal conductivity of the rock type possessing higher porosity values (fractured and altered). Other parameters also depicted either positive or negative monotonic relationships. Significant associations were observed for all parameters when considering the full range of porosity values across all rock types (0-30 %), however, no associations were identified within the individual porosity intervals (0-3 %, 3-6 %, 6-9%, and above 9 %). For all rock types (0-30 %), the association between porosity and both acoustic impedance and compressional wave velocity was successfully quantified, whereas the association between thermal conductivity and seismic wave velocities could not be quantified.

Keywords: Geothermal energy, seismic wave velocities, thermal conductivity, statistical analysis

Table of Contents

Symbols and abbreviations.....	5
Section 1. Introduction.....	6
1.1. Problem Statement.....	8
1.2. Aims and Objectives.....	8
1.3. Research Questions and Hypothesis.....	9
1.4. Scope and Limits.....	11
Section 2. Theory.....	13
2.1. The architecture of a Fault zone.....	13
2.2. Deformation controlled by elastic properties.....	14
2.3. Elastic wave velocities.....	15
2.4. Acoustic and Shear Impedance.....	16
2.5. Thermal Properties in Geothermal Energy.....	17
2.6. Phonon Conduction Theory.....	18
2.7. Porosity.....	20
Section 3. Literature Review.....	22
3.1. Relationships between seismic wave velocities and physical properties of rock.....	22
3.2. Effects of hydrothermal alteration on petrophysical properties.....	24
3.3. Fractures and Conductivity for Geothermal Fluid Movement.....	25
Section 4. Research Materials and Methods.....	27
4.1. Sample Selection and Preparation.....	27
4.2. Laboratory Techniques for Data Collection.....	30
4.2.1. Seismic Wave Velocities.....	30
4.2.2. Density.....	32
4.2.3. Thermal conductivity.....	32
4.2.4. Porosity.....	33
4.3. Statistical analysis.....	33
4.3.1. Spearman's Rank Test.....	34
4.3.2. Chi square test.....	36
4.3.3. Fisher exact test.....	37
4.4. Regression Analysis.....	38
Section 5. Experimental results.....	39
5.1. Scatter Plots.....	39
5.2. Regression Analysis Results.....	45
Section 6. Discussions.....	48
Section 7. Conclusions.....	50
Section 8. References.....	52
Appendix A.....	59
Appendix B.....	60

Symbols and abbreviations

Symbols

Symbol	Meaning
E	Young's modulus
ν	Poisson's ratio
G	Shear modulus
K	Bulk modulus
V_p	Compressional wave velocity
V_s	Shear wave velocity
M	Compressional wave modulus
ρ	Density
λ	Thermal conductivity
Φ	Porosity
q	Heat flow density
L	Specimen length
r_s	Spearman's rank coefficient
n	Number of observations
p-	Probability value
t'_s	Statistical value
t_c	Critical value
ε	Strain
τ	Shear stress
θ	Deforming angle
P	Compressional wave velocity
S	Shear wave velocity
L_p	Phonon mean free path
V_m	Phonon mean velocity
Γ	Scattering rate
P'	Applied pressure
C_V	Lattice specific heat per unit mass
L_p	Phonon mean path
V_m	Phonon mean velocity
v_p	Pore volume
v_t	Bulk volume
v_s	Grain volume

Abbreviations

Abbreviation	Meaning
AI	Acoustic Impedance
SI	Shear Impedance

1. Introduction

Ambitious initiatives toward renewable energies, such as the United Nations' Sustainable Energy for All (2024) initiative and the European Green Deal (2021), have been put into overdrive with the new consciousness on climate change. Scientific consensus, growing public demand, and escalating climatic impact are driving such a shift, thus striving for a low-carbon, resource-efficient, climate-resilient, and carbon-neutral energy system.

Many countries have conventional geothermal resources in their portfolio of energy, either for the generation of electricity or for direct heat applications (Figure 1). The growing need for sustainable and decentralized energy solutions has led to a considerable rise in interest in unconventional geothermal resources in recent years, particularly in deep crystalline settings impacted by faults and fractures. The vast majority, over 80 % of the Earth's internal heat, is contained in the deep subsurface, at depths greater than 5 km. (Jolie et al., 2021)

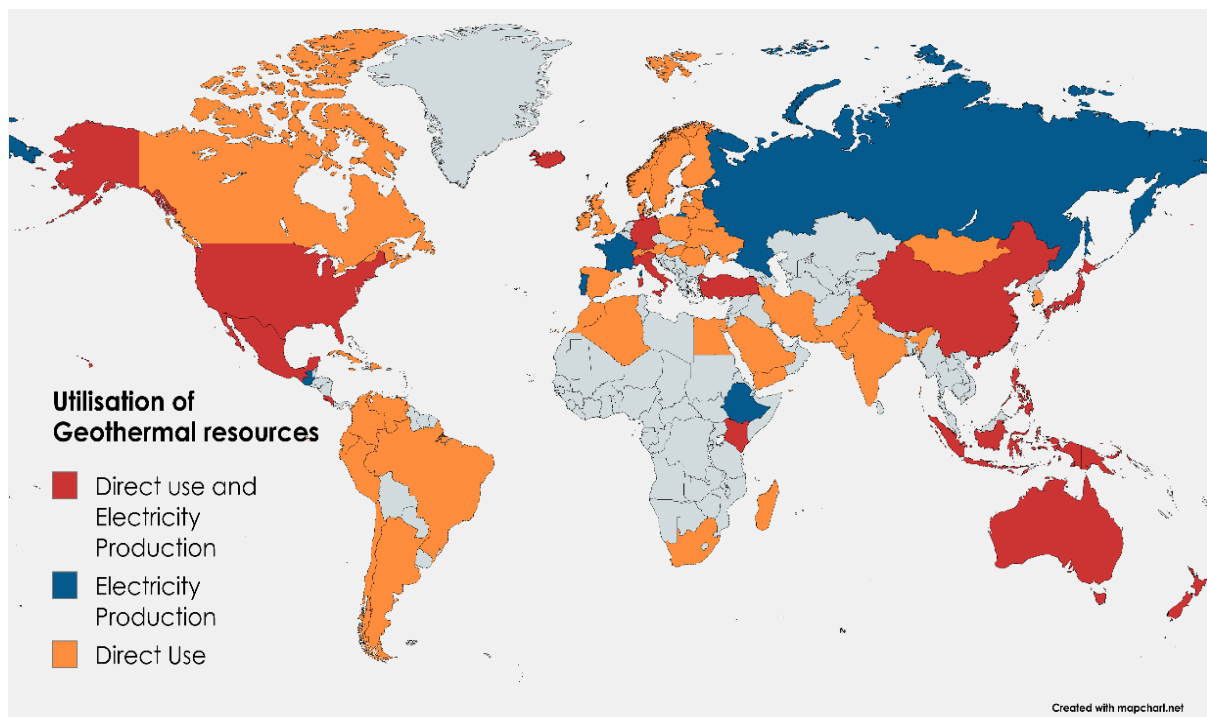


Figure 1: Countries utilizing geothermal resources for direct use, electricity production, or both. *Source: Geothermal Power Database (2015) and created with mapchart.net.*

The potential to generate electricity from geothermal heat other than that bound by the current geological constraints (reservoir quality and advanced drilling technologies) provides an option to supply carbon-free, renewable baseload power on

a global scale (Cascade Institute, 2024). According to the Annual Financial Commitments in Renewable Energy (2023), an estimate of thermal energy (heat generated due to Earth's internal processes like radioactive decay of elements and residual heat from the Earth's formation) stored in 3–10 km from the surface could supply up to 2,000 times the 3.13 TW of electricity equivalent energy demand of the US. Despite this potential, geothermal energy attracted only 200 million USD out of 499 billion USD global renewable energy investments in 2022. As a result, less developed technologies like geothermal energy will require more funding to reach their full potential. This is particularly important given that geothermal energy is a reliable and continuous source of power, eliminating the need for energy storage systems or backup power plants (Geothermal Energy, 2022).

Novel drilling and reservoir-enhancing technologies, such as deep directional drilling techniques and Enhanced Geothermal Systems, are progressing outside typical volcanic and rifting settings. For example, the United Downs Geosystem project in the United Kingdom (Farndale et al., 2022) and Project Red in Nevada (Caliber, 2024). The commencement of such projects indicates that it is economically viable to generate heat from naturally occurring or artificially created fractured reservoirs, thus extending geothermal to regions that the energy industry has traditionally overlooked. (Kauppinen et al., 2020)

The Fennoscandian Shield, also known as the Baltic Shield, comprises Finland, Norway, Sweden, and a part of northwestern Russia. The bedrock dates from the Proterozoic (2500–1300 Ma) and Archaean (3100–2500 Ma) ages. Granites, gneisses, and other metasedimentary or metavolcanic lithologies characterize the crystalline bedrock. Typically, the geothermal gradient is cited as 8–15 °C/ km, suggesting that depths of 6–8 km are required to reach 100°C temperatures. However, as discovered in the St1 deep heat flow project, this estimate is outdated, and the temperature exceeded 200°C at depths of about 6 kilometres (Kukkonen & Pentti, 2021).

About 27.1 % of Finland's total energy consumption is related to space heating (Energiateollisuus ry, 2023). Nearly 4,000,000 TWh of thermal energy is thought to be available in the crystalline bedrock at depths of 4–7 km, which would be sufficient to cover the country's district heating needs for nearly 100000 years (GTK, 2022). Annual average air temperatures at ground level vary from 5°C in the southern part to -2°C in the northern part of Finland. The average temperature of the air varies for different countries and areas in this region (Kukkonen, 1999).

1.1. Problem Statement

Shear impedance, rock porosity, acoustic impedance, acoustic wave velocities, rock density, thermal rock conductivity, and seismic velocities are important factors in most geothermal applications (stimulated geothermal systems and geothermal reservoirs). (Alameedy et al., 2022; Caspari et al., 2020; Weydt et al., 2022)

Physical characteristics of rocks, such as density, porosity, and thermal conductivity, have been shown to affect seismic wave velocity in earlier studies. Seismic wave velocities decrease with increasing porosity; nevertheless, they increase with increasing rock density and decrease with decreasing porosity. Additionally, it has been reported that increased thermal conductivities can increase the velocities of seismic waves. (Mielke et al., 2017; Wyering et al., 2014; Wang et al., 2009; Hartman et al., 2005; Popov et al., 2003; Starzec, 1999; Kukkonen & Peltoniemi, 1998)

Furthermore, it is uncertain how these physical characteristics behave in crystalline bed rocks that are penetrated by faults and fractures, particularly concerning the nature of the correlation and linear relationship between seismic wave velocities and thermal conductivity. Furthermore, Kokkonen and Peltoniemi's (1998) study of Finnish crystalline rocks found no correlation or linear relationship between them.

However, the influence of secondary porosity, such as fracture brought on by mineral dissolution, is ignored in these studies, which concentrate on low porosity and low permeability rocks. Furthermore, a clear association between thermal conductivity and compressive wave velocity was observed for rocks with relatively greater porosity values, including sandstones and volcanoes, but not for plutonic rocks (Mielke et al., 2017). Additionally, a thorough assessment of the petrophysical properties of fractured and changed crystalline formations in Finnish crustal fault zones with high porosity values (up to 30%) was conducted by Bischoff et al. (2024). From the perspective of geothermal energy resources, these areas are currently unexplored.

This information gap makes it difficult to simulate geological behaviour for energy extraction and effectively characterize unconventional geothermal reservoirs. If these relationships are not well understood, geothermal projects will be impractical because of wastefulness and inefficient resource exploitation. (Mielke et al., 2017)

1.2. Aims and objectives

This thesis aimed to investigate the relationship between seismic wave velocities, acoustic impedance, and shear impedance with petrophysical properties such as thermal conductivity, porosity, and density of crystalline rocks of Finland transversed

by faults and fractures. The studied rocks were categorized as massive (host), brecciated, fractured, and altered. Parameters, i.e., thermal conductivity and seismic wave velocities, are addressed in greater depth in this study as compared to others. Literature to date, such as Kukkonen & Peltoniemi (1998), Mielke et al. (2017), Hartman et al. (2005), Popov et al. (2003), and Starzec. (1999) would suggest a negligible or zero correlation of seismic wave velocities with thermal conductivity for low-porosity crystalline rocks. However, a relationship was observed by Mielke et al. (2017) for porous rocks like volcanites and sandstones. This study was conducted to investigate whether a correlation existed between thermal conductivity and seismic wave velocities in crystalline rocks with high porosity resulting from alteration and fracturing.

This study will try to fill the knowledge gap by gaining an adequate understanding of petrophysical characteristics and seismic wave velocities in this type of zone and evaluating how they relate to thermal conductivity, which has not been discussed in the literature for the Fennoscandian Shield.

Establishing a relation between seismic wave velocities and thermal conductivity would allow better modelling of subsurface properties in geothermal reservoirs, especially where fractured and altered crystalline rocks are common. It can also enhance visibility in the subsurface to delineate faults through the application of seismic reflection techniques, as both properties are sensitive to variations in fluid content, porosity, and mineral alteration associated with fault zones, thus improving the detection and mapping of fault zones.

1.3. Research Questions and Hypothesis

Question 1

Do the response variables (P-wave velocity, S-wave velocity, acoustic and *shear* impedance) correlate with the explanatory variables (porosity, thermal conductivity and density), *and can the correlation be quantified?*

For crystalline rocks, hydrothermal alterations, fractures, and faults play a vital role in fluid flow and storage instead of primary porosity alone. The porosity and permeability values are higher than average in this study, which makes it an exceptional case for crystalline rocks, with increased fluid movement and heat transfer. Understanding the correlation and relationship of such variables in this scenario could help to define the reservoir quality of hydrothermally altered and faulted zones.

Hypothesis 1

The response variables and explanatory variables will exhibit a correlation and will depict either monotonic positive or negative relationships. seismic wave velocities and thermal conductivity will possess a significant relationship in this study due to higher porosities.

In contrast to earlier findings, there is no significant correlation across seismic wave velocities and thermal conductivity in crystalline rocks having low porosity, a strong relationship will exist between the response and explanatory variables when examining the crystalline rocks—within a fault zone, as seen in Figure 2 since they possess porosity and permeability values which is more than the average observed for crystalline rocks.

Question 2

How do these relationships vary for different categories of crystalline rocks due to hydrothermal alteration and faulting? i.e., massive, brecciated, fractured, and altered rocks?

Upon establishing such relationships, it will help in understanding the most suitable locations for geothermal energy exploration, better exploration strategies (targeting high temperature zones), and improved reservoir management.

Hypothesis 2

The relationships will get stronger when going from massive to altered rock types. Massive rocks (host rocks) represent the original crystalline rock, i.e., not affected by any process and thus having low porosity values. Contrarily, brecciated, fractured, and altered rocks are affected by hydrothermal alteration and faults.

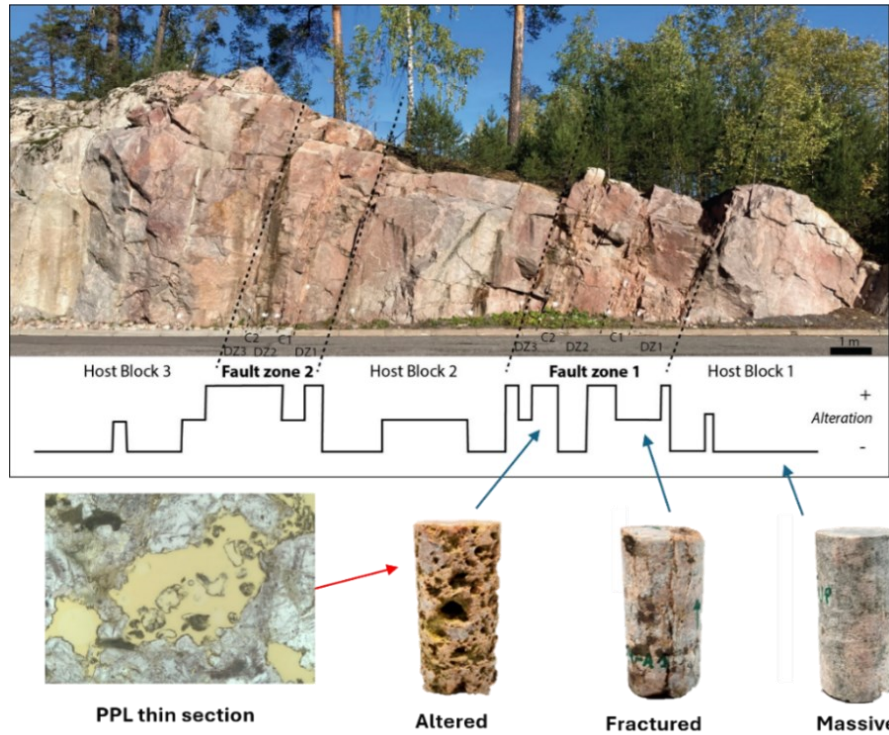


Figure 2: Example of a fault zone in Finland and its association with fracturing and mineral alteration, as observed in an outcrop. Source: Bischoff et al. (2025)

1.4. Scope and Limits

This thesis will primarily focus on determining the correlation across seismic wave velocities and thermal conductivity in fault and fracture zones, with emphasis on crystalline rocks. The impacts of density and porosity on seismic wave velocities and impedances will also be considered as a secondary goal of this thesis. Additionally, the effect of factors like fluid content, temperature, and stress conditions is not considered.

The data of seismic wave velocities through water-saturated rock samples was obtained from the laboratory of Oy Rock Physics Finland, which used ultrasonic testing methods to conduct the measurements at ambient temperature and pressure conditions. Complementary data for the same rock samples, including density, porosity, and thermal conductivity, were obtained from the Deep-HEAT-Flows (2024) project. This study did not include laboratory measurements; it focused solely on statistical analysis conducted using available data.

The relationships and associations between these variables for low enthalpy crystalline rocks comprising granites and gneisses in several key locations of Finland, including Otaniemi, Koillismaa, Kivetty, Mäntsälä, Loviisa, Vantaa, and Kopparnäs, were

studied. These locations depicted higher values of porosities due to the presence of fault and fracture zones. Such analysis can aid in predicting subsurface heat distribution without the need for direct measurement at every location. Moreover, such relationships can identify highly productive geothermal zones, which often correspond to porous formations. This study is also effective in terms of designing efficient wells by mapping fluid pathways in geothermal wells. Also, such relationships can help in selecting an optimized drilling site, thus reducing the financial risks.

Section 1 explains the problem, the research questions, and the hypothesis made. Section 2 consists of basic theory related to fault architecture, petrophysical properties, elastic wave velocities of rocks, and statistical tools used for analysis, along with the key concepts and relevant equations.

Section 3 comprises the literature associated with this subject, and Section 4 discusses the research methodology for this study. It provides an overview of the experimental techniques as well as the concept of statistical analysis tools applied in this study.

Section 5 represents the results of the statistical analysis. Section 6 correlates the findings with previous research on seismic wave velocities, thermal conductivity, and petrophysical properties of rocks. It examines how the observed trends align with existing studies, highlighting agreements and discrepancies of petrophysical variation across the original, altered, and fault zones. Section 7 contains the summary of the results and work carried out in this project.

2. Theory

This section of the thesis explains the theoretical concepts regarding the architecture, formation, and types of faults, as well as various parameters that affect the formation of faults. This section also explains the concept of response variables, including elastic wave velocities, acoustic, and shear impedance. The explanatory variables of density, porosity, and thermal conductivity have been explained as well.

2.1. The architecture of a Fault Zone

Developing predictive solutions to issues surrounding the use of geothermal energy resources requires an understanding of how brittle zones emerge and impact fluid flow. Fault and fracture networks are regarded as crucial structural elements in geothermal systems for fluid circulation, heat transfer, and reservoir permeability. (Haneberg, 1999)

In the Earth's crust, a fault is a fracture /zone of fractures where rocks on either side have shifted relative to one another due to tectonic forces. Faults arise when tension in the Earth's crust surpasses the rock's strength, forcing it to fracture and shift. Faulting is important in many geological processes, including geothermal reservoir formation (Stawikowski, 2017). It is distinguished by high strain localization, which means rocks break and slip along the fault because of the concentrated strain in this narrow area.

Brittle faults have been differentiated based on two key structural domains, which is the fault core and damaged zone. Figure 3 shows the fault core and damage zones surrounding the core (Choi et al., 2015). The fault core, which accommodates majority of the fault displacement, is the central region of a fault where significant rock deformation results from strong shearing. (Haneberg, 1999)

Relatively low strain and less intense deformation or lower bulk shear strain differentiate the damage zones from the fault core (Haneberg, 1999). These contain a variety of subsidiary structures such as subsidiary faults, veins, fractures, and locally fault-related or drag folds. Damage zones are typically characterized by lowered permeability compared to fault core, except where fractures dominate (Choi et al., 2015). Heterogeneously distributed strain typically characterizes the damage zone, which results in anisotropy and heterogeneity in the permeability framework of the damage zone (Bruhn et al., 1994).

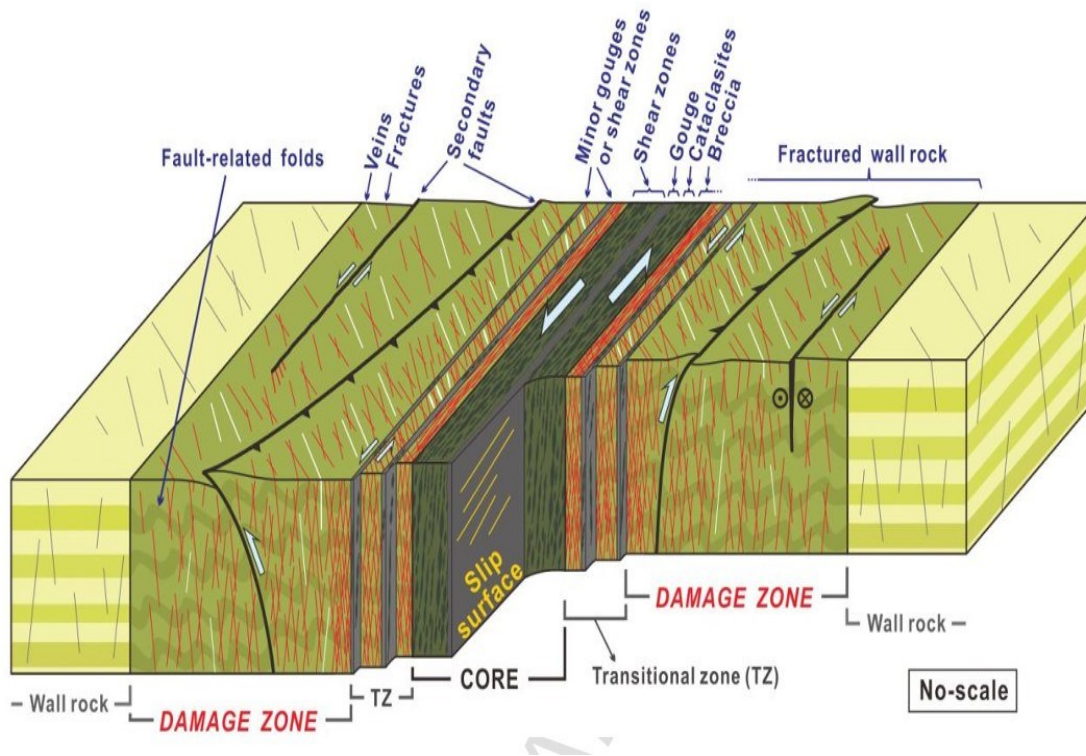


Figure 3: Visual representation of a brittle fault structure. *Source: Choi et al. (2015)*

2.2. Deformation controlled by elastic properties

Important mechanical properties such as Shear modulus, bulk modulus, young's modulus and P-wave modulus can influence the faults and changes in geological materials. These properties influence the way rocks react to stress, strain, and deformation, which in turn affects the formation and spread of faults as well as the material's ability to adjust to variations in pressure, volume, and shear.

2.2.1. Bulk Modulus

Bulk modulus is the impedance of a material to regular volumetric compression. It can be described as the fraction of applied pressure (or hydrostatic stress) to the consequent comparative decrease in volume or volumetric strain.

$$K = \frac{\text{stress}}{\text{strain}} = \frac{P'}{\frac{\Delta v}{v}} \quad (1)$$

K represents the bulk modulus.

P' denotes applied pressure.

$\frac{\Delta v}{v}$ represents the volumetric strain.

2.2.2. Shear Modulus

Shear modulus or Lamé's second parameter characterizes the resistance of a material to shear distortion. It is described as the fraction of shear stress to the shear strain, tangent of a deforming angle θ :

$$G = \frac{\tau}{\tan\theta} \quad (2)$$

Here G represents Shear modulus.

τ represents Shear stress.

2.2.3. P-Wave modulus

P-wave modulus (M) is the resistance of a material to deformation by a longitudinal wave. It defines the impedance of the material to the bulk and shear deformation under compressional waves and is described as a fraction of stress to strain in a uniaxial strain condition. This can be mathematically presented by Equation 3.

2.3. Elastic wave velocities

Mechanical waves are generated when a portion of a deformable medium is compelled to move. Movement of this part of a medium generates deformation in the material and transmits disturbance from one place to another, allowing the wave to travel through the medium. Waves must overcome material resistance and inertia to propagate. Mechanical waves are characterized by energy transmission through particle motion. (OpenStax, 2016)

Since P-waves, also identified as primary waves, are the quickest seismic waves, they arrive at seismic detectors first. By compressing and expanding the substance they pass through, compressional or longitudinal waves move particles in the same direction as the wave. Their "push-pull" motion enables them to travel through both solids and liquids, making P-waves highly effective for subsurface imaging. S-waves,

or secondary waves, always travel slower than P-waves. These are transverse or shear waves that move particles perpendicular to the direction of wave propagation in a side-to-side or "shearing" motion. S-waves can only pass through solids because liquids lack the shear strength necessary to sustain S-wave transmission, in contrast to P-waves, which can pass through liquids (Shearer, 2019). S-waves cannot pass through liquids because they have a shear modulus of zero, which is equivalent to an S-wave velocity of zero. Instead, part of the energy can be converted into P-waves and then back into S-waves.

Three important elastic parameters describe seismic properties, namely, the Shear modulus (G), bulk modulus (K), and P-wave modulus (M). Both P-waves and S-waves will travel at velocities depending on the density, ρ , of the material as well as on its shear and compressibility moduli. Moreover, P-wave velocity increases with increasing shear and compressibility moduli but decreases with an increase in the material's density. It is represented mathematically with the help of equation (3).

$$V_p = \sqrt{\frac{K + \left(\frac{4}{3}\right)G}{\rho}} \quad \text{or} \quad V_p = \sqrt{\frac{M}{\rho}} \quad (3)$$

S-wave velocity increases with increasing shear modulus and decreases with density. It is not affected by compressibility and may be calculated using only two parameters as represented by equation (4).

$$V_s = \sqrt{\frac{G}{\rho}} \quad (4)$$

Here V_s represents Shear wave velocity.

The shear modulus affects the S-wave velocity but also affects the P-wave velocity; materials with lower stiffness have slower P-wave speeds.

2.4. Acoustic and Shear Impedance

Seismic impedances are the product of seismic wave velocities and densities. The resistance a substance provides to seismic waves is referred to by this generic phrase. Seismic impedance is commonly measured in $\frac{kg}{m^2.s}$.

Several variables, including fluid content, lithology, cementation (an important process in rock formation in which dissolved minerals precipitate and bind sediment grains together), and porosity, affect seismic impedances. Porosity generally reduces

resistance; however, the effect varies depending on fluid saturation and pore geometry. As porosity increases, seismic impedances decrease.

Acoustic impedance is applicable to compression waves that oscillate parallel to the material's particles. Additional factors such as porosity, grain contacts, and stiffness may affect the propagation of the wave. It can be expressed mathematically with equation (5).

$$AI = V_p \rho \quad (5)$$

Here, AI represents the acoustic impedance, V_p stands for P-wave velocity and ρ is the density.

On the other hand, shear impedance is related to transverse or shear waves and can be expressed mathematically with equation (6).

$$SI = V_s \rho \quad (6)$$

Here, SI represents the shear impedance, V_s stands for shear velocity and ρ represents the density.

2.5. Thermal Properties in Geothermal Energy

Understanding subsurface thermal behaviour governing the generation, storage, and transport of geothermal energy is central to geothermal energy research and development. An intimate knowledge of such parameters is necessary for the potential of possible geothermal reservoirs, optimization of energy recovery, and system design. High-resolution thermal property characterization overcomes the complexity added by heterogeneous rock geometry by incorporating field measurements, numerical modelling, and laboratory testing. (Kukkonen & Peltoniemi, 1998; Mielke et al., 2017) There are three thermal parameters in geothermal research such as thermal diffusivity, specific heat capacity (C_p) at constant pressure, and thermal conductivity. Wherever there are regions of a body at different temperatures, heat flows from the hot to the cold region. Heat flow can be carried out by three modes: convection, conduction, and radiation. In solid rocks, the heat transport mechanism is by conduction, and above 1200°C it is by radiation.

By Fourier's law, conduction dominates in dense, impermeable, low-porosity rock types, i.e., metamorphic and most plutonic rocks, which are the brecciated or massive rocks in this investigation. Convection dominates permeable materials, e.g., fractured rocks with open or unfilled fractures (Mielke et al., 2017). Heat transfer through lattice vibration or Phonon conductivity is the primary mechanism of heat conduction in

crystalline rocks (Hadley, 2011). The subject of phonon conduction is described in more detail in Section 2.6.

There are two ways to test thermal conductivity: direct and indirect. Direct or laboratory-based techniques include transient techniques like the hot wire and transient plane source (TPS) methods, which are frequently employed in rock and soil studies, as well as steady-state techniques like the guarded hot plate and heat flow meter (Clauser & Huenges, 1995). Additionally, indirect methods are used to measure thermal conductivity. For example, empirical models use characteristics like density, porosity, and mineral composition to predict thermal conductivity in geothermal and geological contexts (Vosteen & Schellschmidt, 2003). Well logging techniques and seismically based estimates can also benefit indirectly from the relationship between heat conductivity and sonic wave velocities and formation factors in underground environments.

Thermal conductivity is a very important property in geothermal modelling, basin and sedimentary studies, and geotechnical applications, because it governs how efficiently heat is transferred through subsurface materials, thus impacting temperature distribution models and energy flow predictions.

The heat flux (q) due to a thermal gradient determines thermal conductivity. As a result, it can be written as:

$$q = -\lambda \frac{\partial T}{\partial z} \quad (7)$$

Here q represents the heat flux.

λ represents the thermal conductivity.

$\frac{\partial T}{\partial z}$ thermal gradient.

The unit of thermal conductivity is $Wm^{-1}K^{-1}$.

2.6. Phonon Conduction Theory

The connection between heat conductivity and compressional wave velocity is explained by phonon conduction theory. It assumes that sonic wave packets, or phonons, propagate along a temperature gradient to carry thermal energy. Cementation, porosity, microfractures, and heat/acoustic wave conduction may interfere with phonon flow, which in turn affects wave velocity and thermal conductivity. (Mielke et al., 2017)

This theory plays a significant role in understanding heat transfer within geothermal reservoirs, particularly for solid rocks that can store and transport fluid. If conduction alone is considered, then phonon transport becomes the dominant mechanism in solid crystalline rocks. Fractures and faults can affect the transport of these phonons. A fracture-free zone, which is less porous and thus has less scattering of phonons, will result in increasing thermal conductivity as compared to a damaged one.

The phonon conductivity theory offers a valid theoretical basis for empirical models that produce precise thermal conductivities for low porosity rocks. A crystalline solid's thermal conductivity is determined by using equation (8).

$$\lambda = \frac{\rho C_v V_m L_p}{3} \quad (8)$$

Here ρ represents density, C_v shows the lattice-specific heat per unit mass, L_p is the phonon mean free path and V_m is the mean phonon velocity. (Williams & Anderson, 1990)

Phonon is considered a unit of energy resulting from vibrating particles in a crystal. Any crystalline solid that consists of atoms bonded together in a fixed three-dimensional space arrangement is termed as a lattice. As the atoms are behaving as if they were connected by small springs, the thermal energy within the atoms or the external forces causes the lattice to vibrate. As a result, mechanical waves are generated within the material that conducts heat and sound. A collection of such waves can propagate through the crystal with given momentum and energy, and therefore such waves can be considered as a component, known as a phonon. (Perkowitz & Sidney, 2025)

Thermal energy in non-metallic solids in the light of geothermal energy reservoirs is primarily carried/transported by phonons. Various scattering mechanisms and material properties can thus affect the efficiency of this heat transport. Ballistic transport mechanisms occur in highly ordered crystals at low temperatures, where the phonons without scattering travel long distances. This process of heat transfer is very rare in natural geothermal reservoirs, as most rocks have microstructural defects. However, for moderate (300-1000 K) to high temperatures (1000-2000 K), in crystalline rocks, the heat is transferred with diffusive transport where the phonons scatter due to defects in the crystal structures and interactions with other phonons. This mechanism is governed by Fourier's law of heat conduction. (Ziman, 1960, Clauser & Huenges, 1995, Chen, 2014)

The average distance a phonon can travel before a scattering event is called Phonon mean free path. A longer mean free path means that the phonon can transport the associated energy for longer distances. This concept is important in understanding the

thermal conductivity and heat transfer for geothermal reservoir rocks. The disruption in the motion of phonons as they pass through rocks is referred to as phonon scattering. Some common scattering processes include phonon-phonon scattering, Phonon-Defect Scattering, and Phonon-Boundary scattering. (Kittel, 2004)

To determine the thermal conductivity, mineral composition plays a vital role as it directly influences the way heat is transferred through the material. The bond strength, density, and atomic structure of minerals contribute to thermal properties. Quartz and Feldspar are examples of minerals that can affect the thermal properties due to their distinct structural characteristics. Quartz is a silicate mineral that has higher thermal conductivity compared to other silicates and is found in abundant quantities in the Earth's crust. The phonons travel more freely through quartz, leading to higher thermal conductivities due to a highly ordered atomic structure with strong covalent bonds between oxygen and silicon atoms (SiO_2). Feldspars, on the other hand, possess a different structure and composition as compared to quartz. Minerals like orthoclase and plagioclase that contain aluminium, sodium, or potassium ions constitute the feldspar group. Moreover, mafic minerals also have higher density than quartz or feldspar, resulting in thermal conductivity values that deviate from minerals like quartz or feldspar. (Clauser & Huenges, 2011)

To assess the geothermal potential of any location, it is important to understand how heat is transferred through the rocks. Phonon conduction theory can be used to explain how heat is transferred through minerals and rocks in geothermal reservoirs. It also explains the temperature and thermal conductivity relationships in detail, which is important to understand heat flow and reservoir behaviour. (Finsterle et al., 2013)

2.7. Porosity

The capability of a reservoir to retain and transfer fluids, which are necessary for heat extraction, is directly impacted by porosity, making it an important rock feature in geothermal energy exploration. By decreasing the shear and bulk moduli of the rock, porosity influences elastic wave velocities, resulting in reduced P-wave and S-wave velocities. Because pores are usually filled with air or fluids, which are less dense than the rock matrix, it also reduces density. (Starzec, 1999)

Porosity is described as the fraction of the pore volume to the bulk volume of the rock.

$$\phi = \frac{\text{volume of pores}}{\text{bulk volume}} = \frac{v_p}{v_t} = \frac{v_t - v_s}{v_t} \quad (9)$$

Here v_p represents the pore volume.

v_t represents the bulk volume.

v_s represents the grain volume.

Porosity is a dimensionless property that can be expressed in percentage or as a fraction. The above definition is related to total porosity, also called absolute porosity. Effective porosity is the fraction of the connected pore volume to the total volume of rock. Connected pore volume, however, depends upon the saturating fluid. (Tiab & Donaldson, 2012)

The term primary porosity defines the volume of void sediment when it is first deposited. The secondary porosity is the extra volume of void derived later. Porosity can be calculated or determined by both direct and indirect methods. The direct or laboratory methods include solid and bulk volume calculations and gas expansion procedures (Heap et al., 2014). Seismic and logging methods are examples of indirect measurements of porosity, since they are based on the relation of porosity to other parameters such as density, neutron response, and seismic wave velocities (PetroWiki, 2024b). Nuclear magnetic resonance techniques can also be applied to evaluate porosity (PetroWiki, 2024).

3. Literature Review

This section represents some of the previous studies conducted on the relationships between the response (Seismic wave velocities and impedances) and explanatory variables (density, thermal conductivity, and porosity). It particularly focuses on the correlation between thermal conductivity and P-wave velocity, previously investigated for low-porosity crystalline rocks and high-porosity volcanites or sandstones. This section also explains studies conducted in terms of hydrothermal alterations and fractures' effects on petrophysical properties like porosity and permeability. It also explains how fractures affect conductivity, and the fluid movement associated with geothermal energy.

3.1. Relationship between seismic wave velocities, porosity, density, and thermal conductivity

A positive correlation was observed between seismic wave velocities and density for 300 crystalline rock samples representing igneous and metamorphic rocks from the southwestern part of Sweden. The study focused on the five rock groups that include gneissic granite, gneissic granodiorite, amphibolite, quartzite, and diabase (Starzec, 1999).

The relationships among thermal conductivity and multiple physical properties of rocks, such as density, porosity, and mineral composition, were investigated experimentally by Popov et al. (2003). The findings showed higher thermal conductivity for denser and less porous rocks, even though the study does not specifically examine the connection between thermal conductivity and seismic wave velocities. This finding is in line with a more common understanding that materials that are denser and less porous tend to exhibit better thermal conductivity and seismic wave velocities.

According to Hartmann et al. (2005), thermal conductivity and seismic wave velocities are related, and thermal conductivity in subsurface formations can be estimated using seismic data. According to their research, since density, mineral composition, and porosity all affect thermal conductivity, higher seismic wave velocities generally correspond to higher thermal conductivity. In the absence of direct measuring techniques, this result gives credibility to the idea that seismic wave velocities can be a useful indirect indicator of thermal conductivity.

Gegenhuber and Schön (2012) investigated the relationship between thermal conductivity and compressional wave velocity, putting forward a novel model that

connects these two characteristics in geological materials. Given that these variables are impacted by physical properties such as density, porosity, and mineral composition, their research indicates that P-wave velocity may serve as a reliable signal for determining thermal conductivity. P-wave velocity is a useful tool for geothermal exploration and subsurface characterization, especially in settings where direct measurements of thermal conductivity are difficult. This relationship is especially helpful in geophysical applications where P-wave velocity is simpler to measure than thermal conductivity.

Kukkonen & Peltoniemi (1998) did not find any evident correlation between thermal conductivity and seismic wave velocities for the 700 water-saturated samples of crystalline rocks at normal room temperature and pressure, however, an inverse relationship between thermal conductivity and density was observed, even though thermal conductivity is theoretically proportional to density. The higher content of quartz in these rock samples is an explanation of this deviation from theoretical predictions, while higher quartz content increases thermal conductivity, it also decreases rock density

A total of 1430 dry rock samples (oven dry) from plutonic (gabbrodiorite, diorite, gabbro, diorite, granodiorite, granite), carbonatic (marl, marble, limestone, dolomite, coquina), clastic sedimentary (arkose, greywacke, sandstone), and volcanic (andesite, basalt, rhyolite) rock types were included in the study conducted by Mielke (2017). The bulk thermal conductivity in this study was measured using an optical scanning method under ambient conditions. A weak or no correlation between thermal conductivity and seismic wave velocities in low-porosity crystalline rocks such as carbonates, volcanites, and plutonic rocks was obtained by Mielke (2017). However, porous rocks such as fine, medium, and coarse sandstones showed a moderate to strong correlation. Mielke (2017) observed a direct relationship between thermal conductivity and compressional wave velocity. Additionally, thermal conductivity and compressional wave velocity in porous rocks showed an inverse relationship with porosity, as both properties tend to decrease with an increase in porosity, and vice versa.

In saturated samples, both thermal conductivity and compressional wave velocity were higher compared to dry samples; this gain was again mainly controlled by porosity. In dry porous rocks, thermal conductivity can be well predicted from compressional wave velocity. However, when the nonporous carbonates and plutonic rocks, except diorite and granodiorite, are considered, no correlation was obtained from which thermal conductivity cannot be feasibly predicted based on acoustic wave velocity. For diorite and granodiorite, a weak correlation was obtained. (Mielke et al., 2017)

Kim et al. (2012) examined three Korean rocks—Asan gneiss, Boryeong shale, and Yeoncheon schist for anisotropic characteristics in thermal conductivities and seismic

wave velocities. The best correlation was observed between P-wave velocity and thermal conductivity, which showed a positive relationship.

3.2. Effects of hydrothermal alteration on petrophysical properties and geothermal energy resources

Hydrothermal alteration is one of the most important processes that can change the properties of reservoirs, especially crystalline rocks. Propylitic and vein alterations in granite reservoirs enhance porosity and permeability. These are very important for enhancing fluid retention and circulation, an important aspect in the utilization of geothermal energy. (Ledésert et al., 2009, Inskip et al., 2023)

According to Bischoff et al. (2024), altered granites can develop up to 20 % porosity and 50 md permeability, which is significantly higher than in unaltered granites. Moreover, Weydt et al. (2022) and Inskip et al. (2023) reported that hydrothermal alterations reduced thermal conductivity and sonic velocities in the Carnmenellis granite and the Los Humeros Volcanic Complex, respectively.

A study of a large shear zone in crystalline rocks in the central Swiss Alps found that hydrothermal alteration caused significant changes in petrophysical properties. These changes included reduced elastic wave velocities and increased porosities, which were notably different from values observed in intact granite. (Caspari et al., 2020)

Alterations can fill the fractures, thus reducing the porosity (silicification). However, some alterations, for example argillic alterations, can increase the permeability because of clay formation that breaks down the structure of rock. Also, the chemistry of geothermal fluids changes due to hydrothermal alteration, and it affects the way they interact with geothermal wells, rocks, and power plant equipment. Thus, understanding this helps geothermal engineers to improve power plant performance by preventing corrosion and scaling in it. Moreover, understanding this concept, especially near fault and fracture zones of the crystalline rocks, can help in identifying high-enthalpy geothermal systems, which are associated with hydrothermal alterations in these zones. Epidote and actinolite alterations (high temperature alterations) mean long-lived and deep heat sources, whereas smectite and kaolinite alterations (low temperature alterations) mean cooler and shallower conditions. (Weydt et al., 2022)

Table 1: Relationship of hydrothermal alteration with response variables (P- and S-wave velocities) and explanatory variables in the literature.

Rock property	Relationship	Author and year
Hydrothermal Alteration and Porosity	Direct relation	Ledésert et al.,2009, Inskip et al., 2023, Bischoff et al., 2024, Caspari et al., 2020
Hydrothermal alteration and thermal conductivity	Inverse relation	Weydt et al., 2022, Inskip et al., 2023
Hydrothermal alteration and Sonic wave velocities	Inverse relation	Weydt et al., 2022, Inskip et al., 2023, Caspari et al., 2020

3.3. Fractures and conductivity for geothermal fluid movement

Fractures and fault zones play a critical role in geothermal reservoir performance. They can influence fluid circulation, control permeability, and impact the efficiency of geothermal energy extraction. The rock permeability and porosity are increased by the presence of faults and fractures, which allows geothermal fluid to circulate. The matrix permeability of rocks in many geothermal systems is low, which makes faults and fractures the primary conduits for fluid movement (Flow et al., 1996). For example, the geothermal fields of Iceland and the East African rift depend on fault-related permeability (Letelier et al., 2020; Omwenga, 2019). Such underground formation traps hot fluid and form geothermal reservoirs. Some faults act as a seal (cap rock) to prevent fluid loss, while others allow continuous fluid circulation. These formations also enhance the efficiency of heat extraction by facilitating convective heat transfer where the cooler fluids sink, and hot fluid rises (Flow et al., 1996). A good example in this case would be the Larderello geothermal field in Italy (Bertini et al, 2018).

A high permeability normally characterizes the major fault zones; this is deduced from the investigations of the Upper Rhine Graben and the St1 Deep Heat project. Fluid flow occurs along faulted or fractured rocks. Hydraulic conductivity, however, is hard to maintain, and substantial reductions in permeability are induced shortly after the stimulation job (a set of different techniques used to improve the permeability for

better heat transfer and fluid flow) (Kukkonen et al. 2023, Frey et al. 2022). Specifically, seismic and ultrasonic studies have shown that fracture porosity is related to wave velocity. In turn, zones with more fractures tend to be more permeable (Starzec, 1999; Caspari et al., 2020).

4. Research Material and Methods

Laboratory measurements of compressional and shear wave velocities were conducted on crystalline rock specimens collected from different fault and fractured zones in southern Finland by Oy Rock Physics Ltd. The seismic wave velocities, along with the supplementary data, i.e., density, porosity, and thermal conductivity for the same samples, were obtained from the Deep Heat Flows (2024) project and were used to conduct statistical analysis in this study. The seismic impedances were calculated using the seismic wave velocities and densities.

The process involved in conducting this study can be seen from Figure 4. It starts with using seismic wave velocity data from the laboratory measurements as an input or starting point. Statistical analysis is then conducted between variables under investigation to determine a monotonic relationship and a linear numerical association. Afterwards, only those variables that depicted numerical association were considered for regression analysis to quantify the associations. The purpose of regression analysis is to come up with a quantified relationship in the form of an equation that can then be used to predict an unknown variable when the other is known.

4.1. Sample Selection and Preparation

Of the 127 specimens obtained from the Deep Heat Flows (2024) research project, 115 samples yielded usable data. These specimens represented different locations of southern Finland, including Skanssi (Turku), Kopparnäs (Inkoo), Porkkala (Kirkkonummi), Ruskeasuo (Helsinki), Laajalahti and Otaniemi (Espoo), Kasavuori (Kauniainen), and Kivetty (Äänekoski). The complete details about the location, rock facies, and fault architecture of all the specimens studied here are presented in Appendix A, but some of these specimens are given in Table 2 for a rough idea.

Process Flowchart

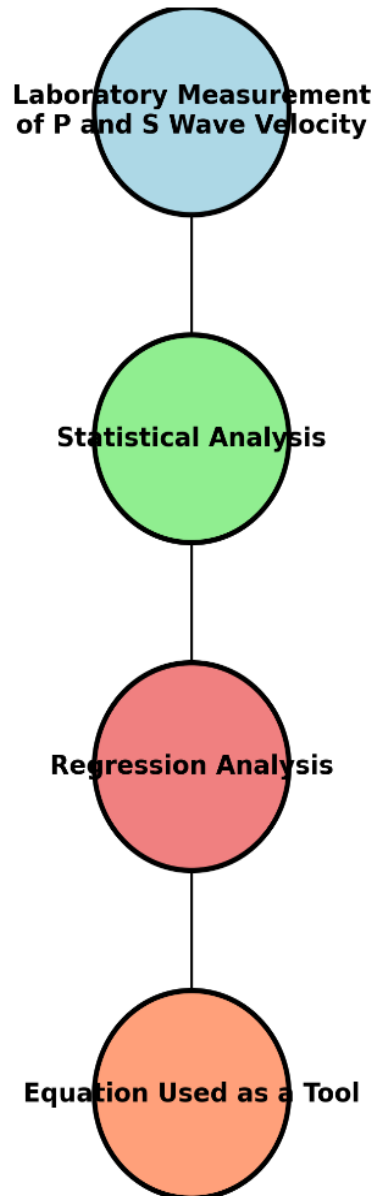


Figure 4: Steps or processes involved in this study. *Source: Produced with Python codes.*

Table 2: Selected samples based on location, rock facies, and fault architecture.

Sample	Location	Rock facies	Fault architecture
FZ2-C2-S001-A1	Skanssi	Altered Migmatite	Fault core
FZ2-C2-S001-C1	Skanssi	Altered Migmatite	Fault core
KOP-D-020-A1	Kopparnäs	Altered gneiss	Fault core
KR1-003	Kivetty	Altered granite	Damage zone
FZ1-C1-S004-A1	Skanssi	Fractured migmatite	Fault core
KOI-002-C	Koillisma	Brecciated granite	Fault core
MHA3-002	Mäntsälä	Brecciated granite	Damage zone
KR4-005	Kivetty	Brecciated granite	Damage zone
KOI-003-C	Koillismaa	Fractured granite	Damage zone
HB5-S001-A1	Skanssi	Massive migmatite	Host block
KUS-001-A1	Vehma	Massive migmatite	Intrusive contact
OTN1-008-A1	Otaniemi	Altered granite	Damage zone
MHA3-001	Mäntsälä	Massive granite	Host block

Specimens were saturated in tap water for 12 days at normal temperature and pressure conditions before the measurements, as seen in Figure 5. This is a bit shorter than the usual 14 days, but with the sample size and porosity higher than usual resulted in early saturation. The core size is irregular; its length in the polished samples is approximately 40 mm.



Figure 5: Selected saturated crystalline rock specimens used for ultrasonic testing. *Source: Oy Rock Physics Ltd.*

4.2. Laboratory techniques for rock property measurements

Data in the form of seismic wave velocities, density, thermal conductivity porosity were analysed statistically. Seismic wave velocities were measured at Oy Rock Physics (Finland) laboratory, whereas density, porosity, and thermal conductivity measurements were conducted at GTK (Finland) and the University of Strasbourg (France) laboratories. The testing methods thus involved are explained below.

4.2.1. Seismic Wave Velocities

Ultrasonic testing systems are one of the prominent standard non-destructive methods used in the characterization of rock materials. It works through the excitation, propagation, and detection of minor waves at ultrasonic frequencies with adjustable pulse lengths. The method of testing does not alter or destroy the sample. The propagation of waves through the material will give important information about properties such as elasticity, density, and structural integrity. This system is used for determining P- and S-wave velocities. A usual configuration of an ultrasonic testing system is schematically shown in Figure 6. (Aydin, 2013)

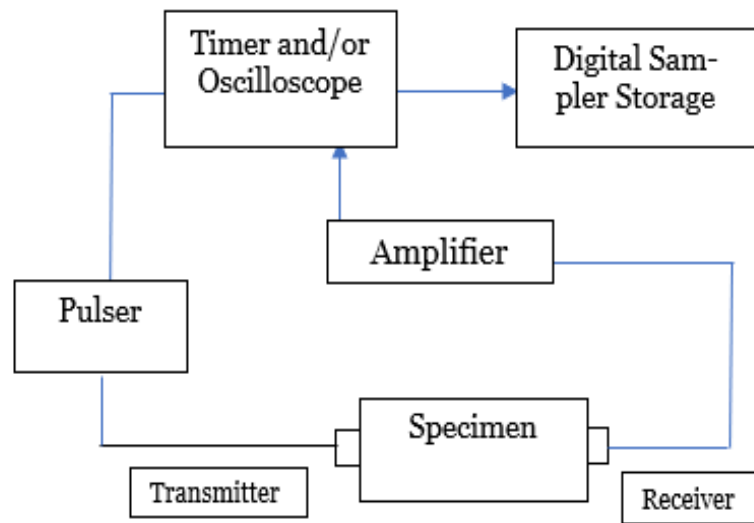


Figure 6: Configuration of a basic ultrasonic testing apparatus. *Source: Aydin (2013).*

In the present study, a frequency of 1 MHz is used to achieve higher signal resolution with good penetration depth. Seismic wave velocities for this study were measured using an Olympus EPOCH 650 with different transducers, such as Olympus V153-RB and V103-RB. Laboratory tests, as seen in Figure 7, were performed according to ISRM 2014 and ASTM D2845-08.



Figure 7: Testing apparatus for measuring seismic wave velocities. *Source: Oy Rock Physics Ltd.*

4.2.2. Density

A digital scale with an accuracy of 0.001 g was used to measure the sample's bulk density at the University of Strasbourg in France using the dry mass. Standard techniques, such as calliper measurements with 0.01 mm accuracy, were used to measure the volume of each regular-shaped sample and fluid displacement for the irregular ones. The bulk density was calculated by dividing dry mass by sample volume.

At GTK's laboratory in Finland, the bulk density of samples was determined by measuring the samples' mass in water and air. A precision scale having 0.01 g accuracy was used to conduct the measurements at 20 °C.

4.2.3. Thermal conductivity

In the laboratory, an approach used to calculate thermal conductivity is the divided bar method. A sample is positioned between copper and quartz discs alternating in a vertical column. Heat flows through the discs due to the temperature difference between the sample and the discs. Once temperature changes in the discs are recorded, thermal conductivity can be calculated using Fourier's law. Another method known as

Transient Plan Source (TPS) can also be used to determine thermal conductivity. Both these methods involve applying a known heat source to the sample and calculating thermal conductivity by measuring its temperature response. (Heap et al., 2020)

At the University of Strasbourg in France, thermal conductivity was calculated with the TPS method that used a Hot Disk 500 Thermal Constants Analyzer. For GTK's laboratory in Finland, a divided bar method was used to calculate the thermal conductivity of the samples in wet conditions.

4.2.4. Porosity

At the University of Strasbourg, a gas pycnometer was used to measure the porosity. This method involves measuring the volume of rock samples by observing pressure changes of helium gas displaced by the sample in a sealed chamber. By combining these volume measurements with the sample's dry mass, the bulk density and porosity are calculated.

For the GTK laboratory, the Archimedean principle was used to measure the samples' connected porosity.

4.3. Statistical Analysis

A non-parametric test was employed for the analysis since the relationship between the variables in this study is expected to be complex and nonlinear, since it is impacted by several parameters such as fluid content, pore structure, and mineral composition.

Non-parametric methods are useful when data fails to fulfil assumptions of normality, independence, or uniformity required for a parametric test (Data Tab, 2024). These statistical tests will help in answering the research questions and hypotheses. Given the non-normal distributions of data, meaning it has been taken from different locations of Finland (non-symmetrical distribution or the data is not clustered around the mean value), these tests are appropriate for answering the research questions with strong statistical inferences. This will determine the relationship between the variables studied, whether correlated, and to what extent.

Figure 8 represents different variables, including seismic wave velocities, seismic impedances, thermal conductivity, density, and porosity, which are investigated in terms of having a monotonic relationship and numerical association with each other. Moreover, Figure 8 predicts the type of relationships between variables in this study. For example, a direct relationship between thermal conductivity and seismic wave velocities, and an inverse relationship between seismic wave velocities and porosity.

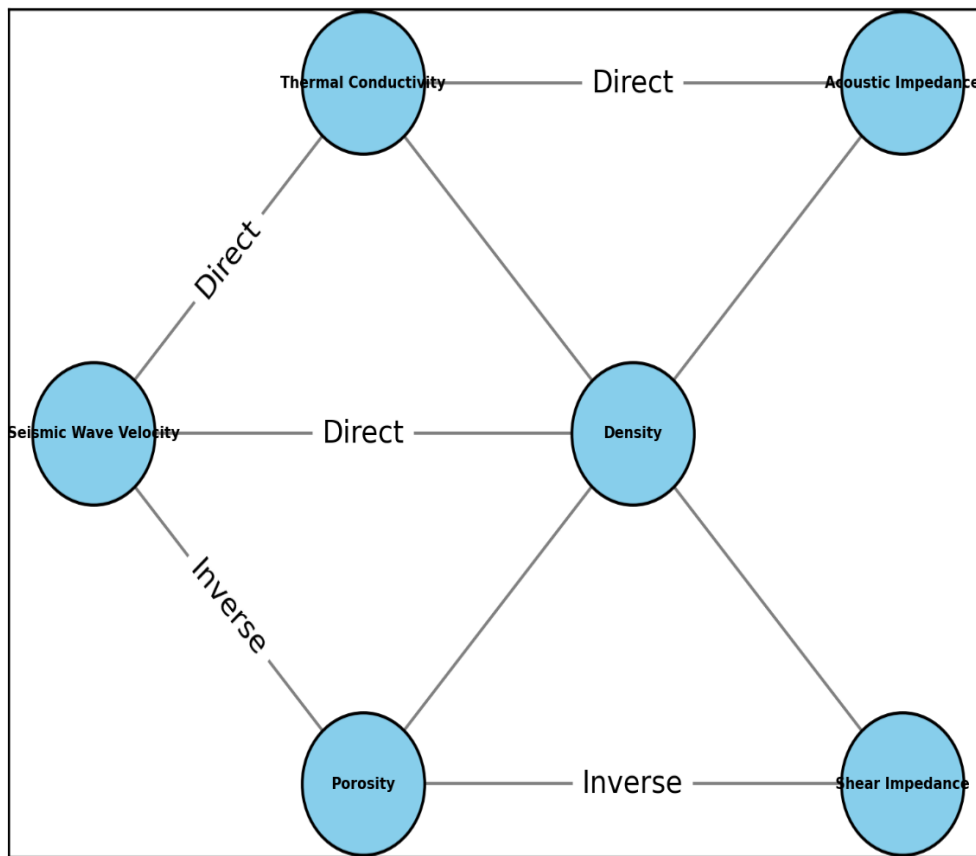


Figure 8: Predicted relationships between the explanatory and response variables based on literature studies. *Source: Produced using Python codes.*

4.3.1. Spearman's Rank Test

Spearman's rank correlation is a statistical test used for testing the association between two variables in a non-linear fashion. It is represented by r_s and gives the strength and direction of the associations between variables when data is ranked or ordered. The important aim of this test is to identify the power and nature of the monotonic relationship between the two variables being compared. The assumptions that precede the use of this test are as follows: Spearman's rank correlation applies in measuring the relationship between ordinal or numeric variables that can be ranked, while not assuming linearity. It is also a non-parametric test, so there is no requirement for a normally distributed data set. (Data Tab, 2024)

Given the complexity introduced by variables like fluid content, pore shape, and mineral composition, a monotonic yet nonlinear connection between the variables is anticipated in this investigation. (Zhao et al., 2021)

Mathematically, it can be written as.

$$r_s = 1 - \frac{6 \sum_{i=1}^n d_i^2}{n(n^2 - 1)} \quad (10)$$

Here d_i = difference in ranks for each pair of values.

n = number of paired observations.

r_s = Spearman's correlation coefficient.

The following interpretations apply to the calculation (Data Tab, 2024).

- If the $r_s = \mathbf{1}$, this means a perfect/strong positive monotonic relationship.
- If $r_s = \mathbf{-1}$, this means a perfect/strong negative monotonic relationship.
- If $r_s = \mathbf{0}$, this means a weak or no monotonic relationship whatsoever.

The Spearman's r value is not that useful in terms of predicting the association between two variables under consideration. It only tells the extent of the monotonic relationship between them. To determine the association, the r_s The value is converted into its statistical value and then compared with its critical value, which is calculated separately. (Data Tab, 2024)

The statistical value for Spearman's rank correlation is calculated from the equation (11).

$$t_{s'} = \frac{r \sqrt{n - 2}}{1 - r^2} \quad (11)$$

Here t'_s represents the test statistic for Spearman's rank correlation, r = Spearman's rank coefficient, and n denotes the number of observations. For the given degrees of freedom ($dof=n-2$) and significance level ($\alpha=0.05$), the critical value for Spearman's rank correlation is calculated using the t-distribution. The variables are said to have a significant association if the test statistic or statistical value is greater than the critical value (t_c).

If $t_{s'} > t_c$, There is a significant association.

If $t_{s'} < t_c$, There is no significant association.

Sample size is an important factor in the outcome of Spearman's rank correlation tests, this can affect the results in our study when categorizing the samples in terms of porosity. A large sample size has a few advantages, as shown by Figure 9.

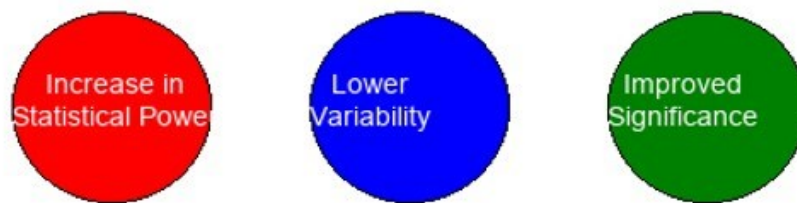


Figure 9: Advantages of a larger sample size on the results of statistical tests. *Source: Produced using Python codes.*

4.3.2. Chi-square Test

This test helps in ascertaining whether the variables are independent of each other. If the p-value is less than the significance level, which is often chosen as 0.05, then the variables are said to be dependent, and the null hypothesis is rejected. If the p-value is greater than 0.05, then the variables are independent. The variables involved must be either categorical or numeric. Chi-square tests work best when the range of observations is limited and expected frequencies are sufficient. For small sample sizes, one expects a weaker reliability in the Chi-square test, because some expected values may drop below the critical value usually accepted as 5. (Field, 2013; Data Tab, 2024)

Since the Chi-square test will only consider data on categories, this study will convert its numerical data into categorical data. It must be done so by a process known as binning, which is carried out with the help of Python codes.

In statistical analysis, binning is the process of dividing continuous data into distinct groups or intervals, frequently to make analysis easier or to better illustrate distributions. (Data Tab, 2024)

4.3.3. Fisher's Exact Test

Fisher's exact test is used to determine whether two binary categorical variables are independent of each other in a contingency table, particularly when the sample sizes are very small. It assumes that the data follow no distribution; hence, it is a non-parametric test. (Data Tab, 2024)

The following are the assumptions of this test:

- The two variables under investigation should be binary; in other words, they will have only one of the two values.

- There should be no relationships between the groups, and the data should be randomly selected.

- There should be one or more cell value counts less than five in the contingency table. If all the values are above five, then the Chi-square test should be performed instead of this.

This test is considered best for small sample sizes and low expected frequencies, and less practical or reliable for large sample sizes. Without using large-sample approximations, it calculates the precise probability of detecting the data under the null hypothesis. Because of this, it is favoured in situations when the expected frequency assumption is not satisfied, or the sample size is limited (Agresti & Finlay, 2018).

In summary, Spearman's rank test is used in this study to measure the strength and direction of the monotonic relationship. This test is also used to determine the numerical association between two variables by comparing their statistical value to its critical value. Chi-square test is used to determine if the variables are dependent or independent from each other, and Fisher's exact test is used for the same purpose, but in case of small sample sizes. The statistical analysis is conducted using Python codes developed for this work, all studied tests were applied in this thesis with the same number of observations (Individual or combined porosity range). The complete code for this analysis can be accessed using the link provided in the Appendix A section of this thesis.

4.4. Regression Analysis

Moreover, regression analysis is undertaken on Microsoft Excel to predict the strength of associations between variables that have been compared and to check whether these associations can be quantified or not. For this process, only those variables are considered that are statistically significant. In this study, for the combined porosity range (0-30 %), all the variables possessed a significant association when compared. A linear regression model has been used for this study. The regression analysis is performed for the response (Seismic wave velocities and seismic impedances) and explanatory variables (density, porosity, and thermal conductivity) investigated in this study across the combined porosity interval (0-30 %).

The R^2 value and the type of fitting for each parameter are also calculated. A statistical metric known as the coefficient of determination, or R^2 , shows how well the data fits a regression model. Excel's linear regression analysis is frequently used to evaluate how strongly variables are related to one another. A value near zero denotes a poor fit, whereas a value near one shows the model explains most of the data variability. The R^2 value is the extent to which changes in the independent variable predict a change in the dependent variable. A greater R^2 value suggests that the model explains most of the variability in the dependent variable and fits the data well. Whereas a lower R^2 value suggests that the dependent variable may be influenced by other factors because the model does not account for most of the variability.

5. Experimental Results

This section of the thesis presents the results of statistical analysis conducted on the samples of crystalline rock transected by faults. It also shows the relationships and numerical association between the response (Seismic wave velocities and seismic impedances) and explanatory variables (Density, porosity, and thermal conductivity). Results of different statistical analysis tools are presented in various porosity intervals, including 0-3 %, 3-6 %, 6-9 %, and greater than 9 %. Results of the general relationship and association between the variables for the combined porosity range (0-30 %) are also given in this section.

5.1. Scatter Plots

Figure 10 (A) represents a scatter plot between compressional wave velocity and thermal conductivity. A positive trend is observed here, i.e., thermal conductivity increases with an increase in compressional wave velocity. It can be observed that for low-porosity rocks in Figure 10 (A), no proper trend between thermal conductivity and compressional wave velocity is observed, whereas a proper trend is observed for higher porosity ranges. i.e., the blue and red points. The shear wave velocity behaves similarly to thermal conductivity, as observed for the compressional wave velocity, a direct positive relationship can be seen from Figure 10 (B). It can also be observed from the scatter plot in Figure 10 (B) that higher porosity values exhibit a good relationship between these two parameters as compared to the lower porosity values.

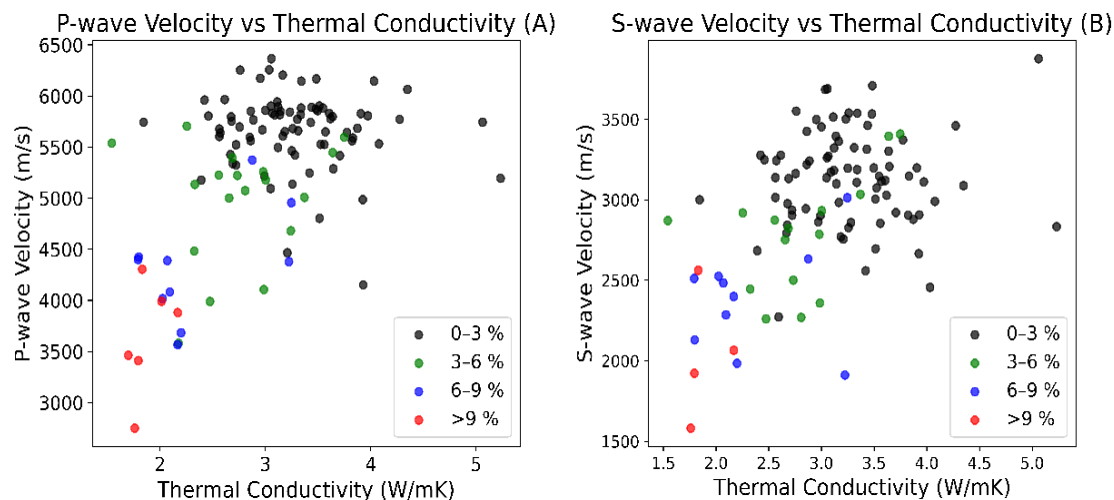


Figure 10: Scatter plot of seismic wave velocities versus thermal conductivity. *Source: Produced with Python codes.*

A positive monotonic relationship is observed between seismic wave velocities and thermal conductivity upon applying Spearman's rank test. With an increase in porosity values, the strength of the relationship increases, as seen in increasing positive Spearman's r values in Tables 3 and 4.

Table 3 represents the statistical and critical values for the Spearman's rank test conducted to determine whether compressional wave velocity and thermal conductivity are statistically significant or not. For individual porosity intervals, no obvious significant association was observed, whereas a significant association can be seen for the combined porosity value (0-30 %). The reason for this association is that Spearman's rank statistical value is greater than its critical value for the combined porosity range, whereas for individual porosity intervals, it is not. A similar observation was found for shear wave velocity and thermal conductivity, as shown in Table 4. For the combined porosity range, statistical and critical values for Spearman's rank tests are thus highlighted yellow in Tables 3 and 4.

The Chi-square statistics and Chi-square critical values are given in Tables 3 and 4, indicating seismic wave velocities are not statistically significant for individual porosity intervals, however, the combined porosity range had statistical values greater than their critical values, thus showing a significant association. For the combined porosity range, Chi-square statistical and critical values are coloured Green in Tables 3 and 4.

Table 3: Statistical test values for compressional wave velocity versus thermal conductivity.

Porosity (%)	0-3 %	3-6 %	6-9 %	Above 9 %	Combined
Spearman's r value	-0.06	0.03	0.1	0.8	0.3
Statistical value (Spearman)	-0.6	0.1	0.3	1.9	3.6
Critical value (Spearman)	2.0	2.2	2.3	4.3	1.9
Chi-square p-value	0.8	0.8	0.1	1	0.01
Statistical value (Chi square)	1.4	1.5	1.5	0	13.3
Critical Value (Chi square)	9.5	9.5	6	3.9	9.5
Fisher exact value	0.6	1	1	0.3	0.1

Table 4: Statistical test values for shear wave velocity versus thermal conductivity.

Porosity (%)	0–3 %	3–6 %	6–9 %	Above 9 %	Combined
Spearman’s r value	-0.1	0.4	0.04	0.8	0.4
Statistical value (Spearman)	-0.7	1.8	0.120	1.9	4.2
Critical value (Spearman)	2.0	2.2	2.3	4.3	2.0
Chi-square p value	0.5	0.01	0.15	1	0.01
Statistical value (Chi square)	3.0	14	3.7	0	14
Critical Value (Chi square)	9.5	9.5	6	3.8	9.5
Fisher exact value	1	1	1	1	1

Figure 11 (A) and Figure 11 (B) represent the scatter plot between seismic wave velocities and thermal conductivity, depicting an inverse relationship. It can be inferred that lower seismic wave velocities can be associated with highly porous locations. Lower porosity intervals show a good relationship, whereas high porosity intervals depict a weak relationship, as the points are more scattered.

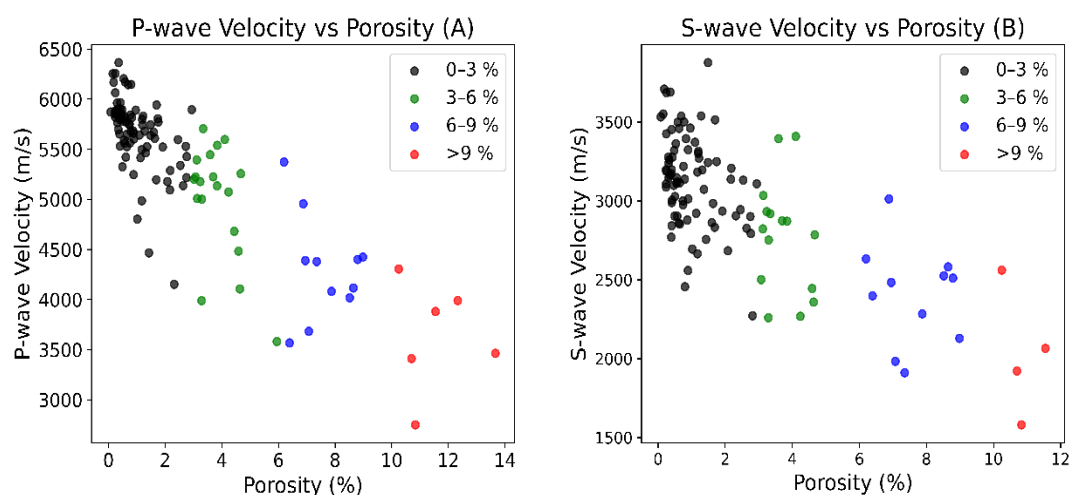


Figure 11: Scatter plot of seismic wave velocities versus porosity. *Source: Produced by Python codes.*

The result of Spearman’s r test, as seen in Tables 1 and 2 of Appendix B, indicates a negative monotonic relationship between seismic wave velocities and porosity. In

terms of significant association between the two parameters, both Spearman's rank and the Chi-square test indicated an association for combined porosity ranges (0-30 %) and nothing for individual porosity intervals. For Spearman's tests, these values are highlighted in yellow colour, and for Chi-square, it is green as shown in Tables 1 and 2 of Appendix B.

Figure 12 (A) and Figure 12 (B) represent the scatter plot between seismic wave velocities and density, depicting a direct relationship of increasing seismic wave velocities with increasing density values, associating higher seismic wave velocities with higher density values.

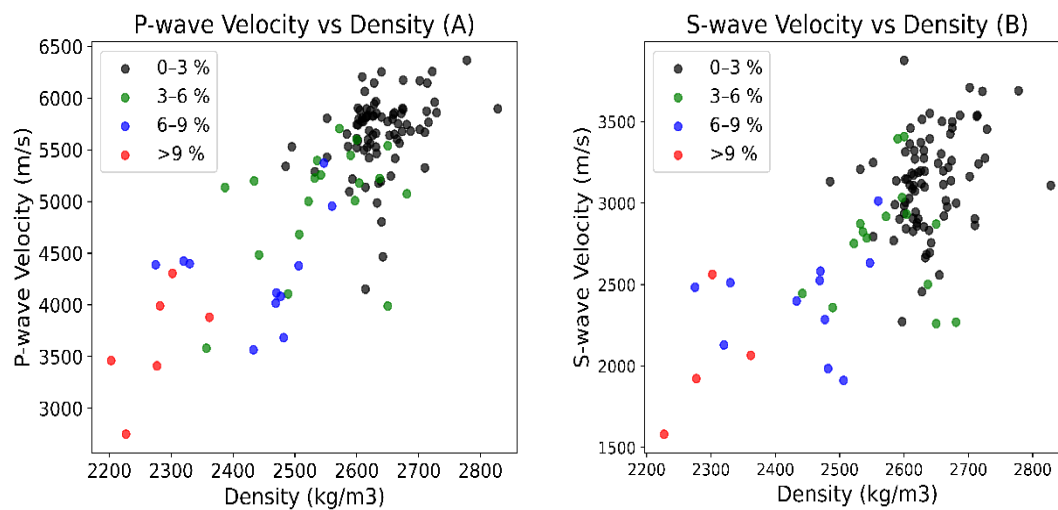


Figure 12: Scatter plot of seismic wave velocities versus densities. *Source: Produced with Python codes.*

The result of Spearman's r test, as seen in Tables 3 and 4 of Appendix B, indicates a positive monotonic relationship between seismic wave velocities and porosity. Tables 3 and 4 of Appendix B also represent the statistical and critical values associated with Spearman's and Chi-square tests. These tests resulted in similar observations to those for the previous parameters. i.e., an association for the combined porosity range and nothing for individual intervals.

Figure 13 (A) and Figure 13 (B) depict a direct relationship between seismic impedances and thermal conductivity, meaning that increasing seismic impedances means increasing thermal conductivity. It is also observed that lower porosity depicts higher values for thermal conductivity and seismic impedances.

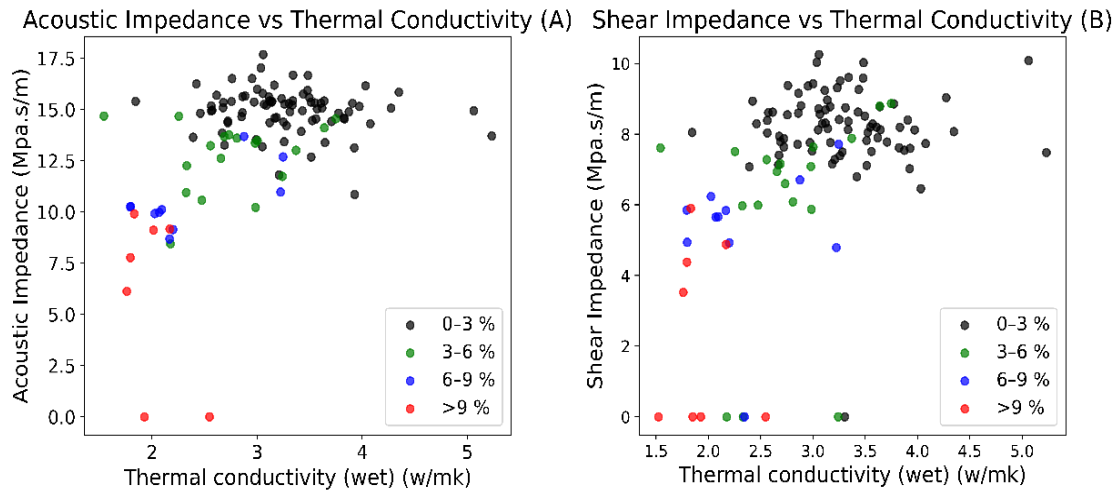


Figure 13: Scatter plot of seismic wave velocities versus thermal conductivity. *Source: Produced by Python codes.*

A positive monotonic relationship is observed between seismic wave velocities and thermal conductivity, as seen in Tables 5 and 6, respectively, which shows a positive value for the combined porosity range. Tables 5 and 6 also represent the statistical and critical values of Spearman’s rank and Chi-square tests. These values predict no significant association for individual porosity intervals. However, for combined porosity values (0-30 %), a significant association is observed. The statistical value for these tests is greater than its critical values, thus showing an association between seismic impedances and thermal conductivity. These values are highlighted in colours, yellow for spearmen and green for Chi-square tests, as shown in Tables 5 and 6, respectively.

Table 5: Results of statistical tests for acoustic impedance versus thermal conductivity.

Porosity (%)	0-3 %	3-6 %	6-9 %	Above 9 %	Combined
Spearman’s r value	-0.1	-0.02	0.3	0.8	0.3
Statistical value (Spearman)	-1.3	-0.03	1.1	1.9	3.3
Critical value (Spearman)	2.0	2.2	2.3	4.3	2.0
Chi-square p value	0.8	0.7	0.02	1	0.001
Statistical value (Chi square)	1.7	1.9	8	0	18.1
Critical Value (Chi square)	9.5	9.5	6.0	3.8	9.5
Fisher exact value	0.2	1	1	0.3	0.3

Table 6: Results of statistical analyses for shear impedance versus thermal conductivity.

Porosity (%)	0–3 %	3–6 %	6–9 %	Above 9 %	Combined
Spearman’s r value	-0.1	0.4	0.1	0.8	0.4
Statistical value (Spearman)	-0.9	1.7	0.2	1.9	4.2
Critical value (Spearman)	2.0	2.2	2.3	4.3	2.0
Chi-square p value	0.5	0.01	0.1	1	0.003
Statistical value (Chi square)	3.0	14	4.4	0	16.41
Critical Value (Chi square)	9.5	9.5	6.0	3.8	9.48
Fisher exact value	0.18	0.6	1.0	0.3	0.03

Figure 14 (A) and Figure 14 (B) relate the acoustic and shear impedance inversely with porosity. It can be seen from the same figures that an increase in porosity values decreases the acoustic and shear impedances and thus has an inverse relationship.

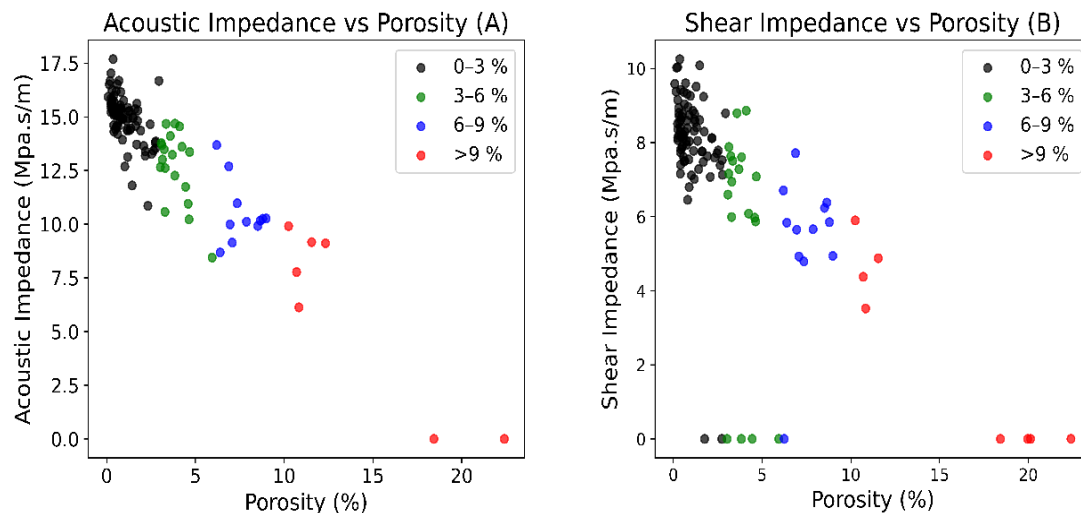


Figure 14: Scatter plot of seismic impedances versus porosity. *Source: Produced by Python codes.*

Moreover, a negative monotonic relationship between seismic impedances and porosity, whose strength increases with increasing porosity values, was confirmed by Spearman’s r value as seen in Tables 5 and 6 of Appendix B. These tables also represent

the statistical and critical values of Spearman’s and Chi-square tests. By comparing these values, it was observed that no significant association between seismic impedances and porosity exists for individual porosity ranges, whereas, for combined ones (0-30 %), a significant association is observed. The statistical and critical values are highlighted like previous parameters.

The relationship type and whether a significant association exists between the response variables (seismic wave velocities and impedances) and explanatory variables (thermal conductivity, density, and porosity) for the combined porosity values (0-30 %) tested by different statistical tools are represented in Table 7. This table gives a summary of the results obtained in this study. It can be seen from the table that all variables in this study, particularly seismic wave velocities and thermal conductivity, depict a good monotonic relationship (Positive/Negative) and have a significant association with each other. The significant association is only observed for the porosity intervals ranging from 0 to 30 %, i.e., the combined porosity values.

Table 7: Summary of results for the parameters compared in this study. Thermal conductivity is denoted by λ , porosity by ϕ , and density by ρ .

Parameter 1	Parameter 2	Monotonic Relationship	Significant Association
P-wave	λ	Positive	Yes
S-wave	λ	Positive	Yes
AI	λ	Positive	Yes
SI	λ	Positive	Yes
P-wave	ϕ	Negative	Yes
S-wave	ϕ	Negative	Yes
AI	ϕ	Negative	Yes
SI	ϕ	Negative	Yes
P-wave	ρ	Positive	Yes
S-wave	ρ	Positive	Yes

5.2. Regression Analysis Results

A linear regression analysis was conducted using Microsoft Excel to examine the relationship between seismic wave velocities (Independent variable) and thermal conductivity (Dependent variable) as shown by Figure 15 (A) and Figure 15 (B). The

R^2 value obtained from the analysis was 0.25 and 0.22 meaning that the equation/model derived from this analysis as shown in Table 8 to calculate the target value of thermal conductivity from the values of seismic wave velocities, does not account for most of variability and the variability in the dependent variables is mostly accounted by other factors rather than seismic wave velocities alone. As a result, this equation cannot be used to predict thermal conductivities from the values of seismic wave velocities. This also means that the strength of the association is weak.

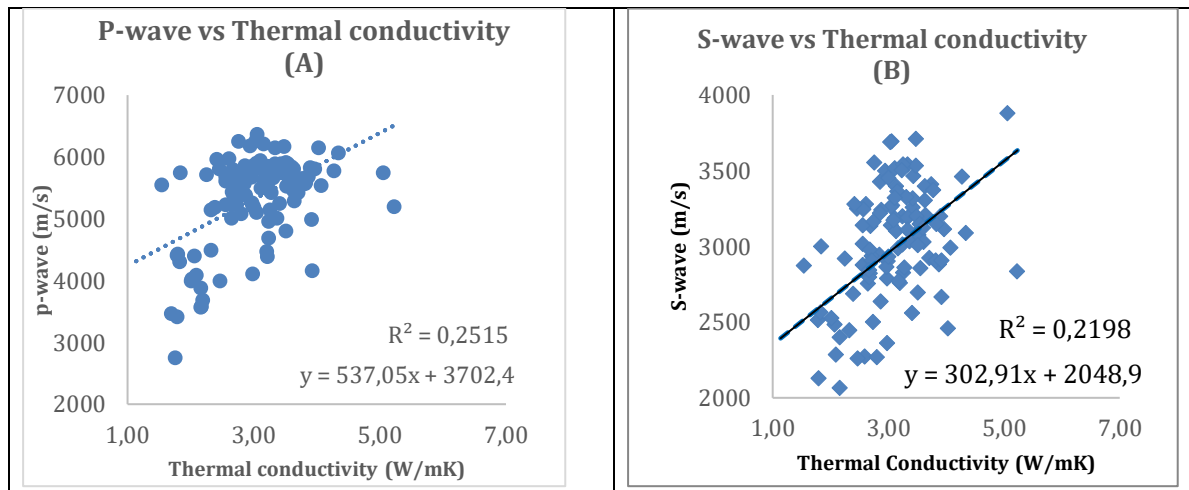


Figure 15: Regression analysis between seismic wave velocities and thermal conductivity. *Source: Produced with Microsoft Excel.*

On the other hand, R^2 obtained from the regression analysis of compressional wave velocity and acoustic impedance with porosity gives values of 0.71 and 0.84 as shown in Figure 16 (A) and Figure 16 (B), meaning that the equations/models highlighted in Table 8 are reliable. The equations can be used to calculate the target value of porosity from the values of compressional wave velocity and acoustic impedance. This means, variability in the dependent variable (porosity) is mostly accounted for by the variability in independent variables (compressional wave velocity and acoustic impedance), thus depicting strong correlations.

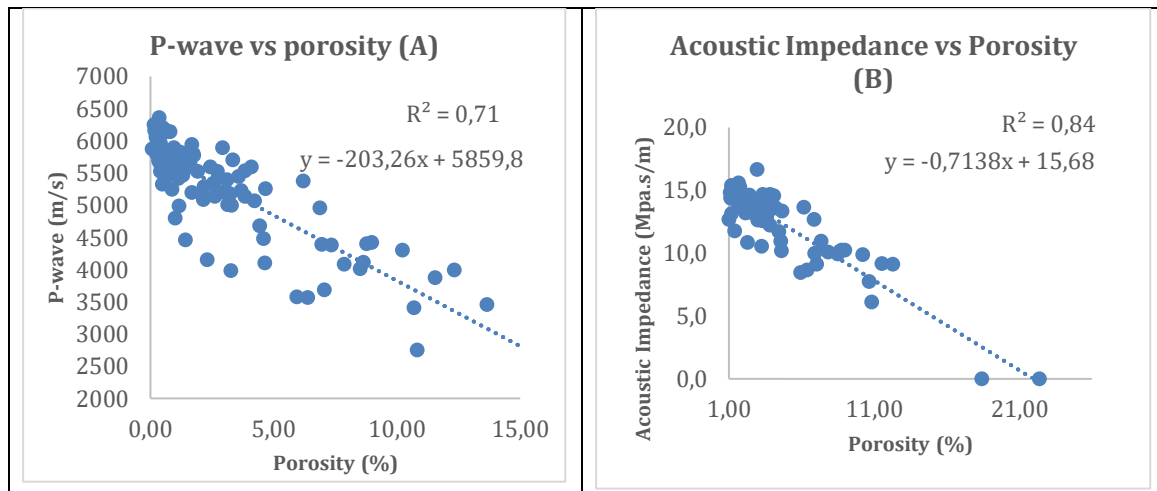


Figure 16: Regression analysis of P-wave velocity and acoustic impedance versus porosity. *Source: Produced with Microsoft Excel.*

Table 8: Results of regression analysis between thermal conductivity (λ), seismic wave velocities (P and S), acoustic impedance (AI), and porosity (Φ).

Parameter 1	Parameter 2	Equations	Fitting type	R^2
λ	P	$\lambda = \frac{P - 3702}{537}$	Linear	0.25
λ	S	$\lambda = \frac{S - 2049}{303}$	Linear	0.22
Φ	P	$\Phi = \frac{5860 - P}{203}$	Linear	0.71
Φ	AI	$\Phi = \frac{16 - AI}{0.714}$	Linear	0.84

The regression analysis conducted on other parameters studied in this thesis can be seen in Figure 1 of Appendix B. The R^2 for the parameters being compared in Table 7 of Appendix B is lower, meaning these models/equations are not reliable to predict the unknown variables from the known ones, and such parameters depict weak numerical association.

6. Discussions

This study suggests a monotonic positive relationship between seismic wave velocities and thermal conductivity for crystalline rock samples taken from the fault and fracture zones of Finland. However, according to I.T. Kukkonen et al. (1997) and Mielke et al. (2017), for low porous crystalline rocks, seismic wave velocities and thermal conductivity were not statistically significant and did not depict a relationship. Additionally, Mielke et al. (2017) observed in their study that for porous rocks (volcanites or sandstones), a relationship and association exist between seismic wave velocities and thermal conductivity. The study conducted in this thesis aligns with the observations of Mielke et al. (2017) in the sense that for high porous crystalline rocks in the fault and fracture zones of Finland, a relationship and significant association do exist. These observations can be seen from Figure 10 (A) and Figure 10 (B) which depicts that for high-porosity intervals, the plot is not much scattered, meaning there is a significant relation, whereas, in case of low-porosity intervals, the plot scatters more (may be due to different mineralogy) and reflects insignificant relation. For the porous rocks, thermal conductivity and seismic wave velocities are largely controlled by the porosity, which in turn depends on the alteration in the rocks. Porosity increases with increasing alteration as the rock changes from a massive state to an altered state (Bischoff et al., 2024). The alteration of rocks in this study results from the faults and fracture zones. This means that if crystalline rocks are more porous, as is in this study (nearly 30 %), a relationship and association should exist between the parameters studied in this thesis, which were not observed for low porous crystalline rocks.

The relationship of seismic wave velocities with porosity and density aligns with the study conducted in the literature. Seismic wave velocities increase with an increase in density and decrease with lower porosity values. Higher values of seismic wave velocities mean higher thermal conductivity and lower porosity values. Higher thermal conductivity can result in more efficient heat transfer, but lower porosity can limit the fluid flow. Thus, it is important to have conditions for a geothermal reservoir that has enough thermal conductivity for heat transfer and enough porosity to transmit that fluid to the surface. The relationship between seismic wave velocities and thermal conductivity, if understood properly, can support various processes involved with geothermal energy systems. For example, in predicting the subsurface heat distribution, identifying highly productive geothermal zones, designing efficient geothermal wells, and optimizing the drilling techniques.

Other relationships in the light of acoustic and shear impedances with thermal conductivity and porosity showed trends as seen in the literature. i.e., with an increase in porosity, seismic impedances and thermal conductivity decreased. Such parameters were not studied for crystalline rocks in fault and fractured zones before. Understanding the relationships between seismic impedances with thermal conductivity and porosity can aid in assessing the efficiency of heat transfer and the

fluid storage capacity of the reservoir. Higher values of seismic impedances suggest dense hot rocks with high heat transfer capacity, whereas low values of seismic impedances mean high porous rocks that can withstand reservoir fluids for hydrothermal circulation.

For a significant association between the parameters compared in this thesis, it was seen that only the combined porosity intervals ranging from 0-30 % showed a significant association, whereas for individual porosity intervals, no significant association existed. The number of observations or the size of the samples is higher in the combined intervals, making it more reliable, and lower in the individual intervals, making it less reliable. This means the number of observations for statistical analysis is higher as compared to the individual porosity intervals. To test the strength of such associations, regression analysis was conducted. This analysis gave lower R^2 values for thermal conductivity and seismic wave velocities, meaning that the strength of the association between these two parameters is not strong, and the equations suggested to calculate thermal conductivity from seismic wave velocities is not reliable. However, the equations derived from the regression analysis to calculate porosity from the compressional wave velocity and acoustic impedance were reliable due to the strong association observed for these parameters in this study.

7. Conclusions

This study investigated the type and strength of the relationship, along with the statistical association and its strength for comparing seismic wave velocities and seismic impedances with thermal conductivity, density, and porosity. A total of 115 samples taken from the Finnish crystalline rocks transected by faults and fractures were investigated, resulting in high values of porosity (nearly 30 %). These specimens represented different locations of southern Finland, including Turku, Inkoo, Kirkkonummi, Helsinki, Espoo, and Kauniainen, and were categorized into five distinct types named massive, brecciated, fractured, altered, and fractured-altered. Seismic wave velocities, density, thermal conductivity, and porosity data were obtained from the laboratory measurements conducted by GTK and Oy Rock Physics Ltd under the umbrella of the Deep Heat Flows (2024) project. Statistical analysis tools, i.e., Spearman's rank, Chi-square, and Fisher's exact tests, were used to conduct this study. These tests on the data were carried out with Python (link to the codes is available in Appendix A) and were used to determine the type and strength of the relationships and their association. Moreover, regression analysis was conducted on these variables to test whether these associations can be quantified or not.

The following were the main findings from this study.

1. A monotonic (positive or negative) relationship was found between the parameters studied in this thesis. The strength of these monotonic relationships increased with increasing porosity values. A positive monotonic relationship was observed between seismic wave velocities and thermal conductivity for crystalline rocks transected by faults. A clear relationship was seen for these two parameters in high-porosity samples as compared to low-porosity ones. Also, the seismic impedances behaved similarly with porosity and thermal conductivity as expected. i.e., high acoustic impedance correlates with higher thermal conductivity and lower porosity.
2. All parameters, including seismic wave velocities and thermal conductivity, compared in this study were statistically significant for the combined porosity interval (0-30 %), and for individual porosity intervals, no significant associations were observed.
3. Equations/Models derived from regression analysis were not reliable for predicting thermal conductivity from seismic wave velocities. Conversely, the equations derived to calculate porosity from compressional wave velocity and acoustic impedance were reliable.

This research has improved our understanding of petrophysical and thermal characteristics in crystalline rocks crucial to geothermal exploration. It examines

monotonic correlations, the intensity and relevance of associations, and their consequences within fault and fracture zones to demonstrate the impact of increased porosity on key petrophysical parameters such as rock density, elastic wave velocity, and thermal conductivity. The petrophysical and thermal variations of these fault zones, which were previously disregarded in the literature, are now recognized as major areas for investigation due to their potential to improve subsurface permeability and heat flow resources. By focusing on these previously unknown interactions between faults and their host rocks, this study helps to identify attractive exploration areas and encourages the development of more efficient geothermal exploration tactics. Furthermore, it delivers reliable, data-driven inputs that are necessary for improving the reliability and precision of geothermal reservoir modelling—critical information for evaluating geothermal resources in crystalline settings.

8. References

- Alameedy, U., Alhaleem, A. A., Isah, A., Al-Yaseri, A., Mahmoud, M., & Salih, I. S. (2022). Effect of acid treatment on the geomechanical properties of rocks: an experimental investigation in Ahdeb oil field. *Journal of Petroleum Exploration and Production Technology*, 12(12), 3425–3441. <https://doi.org/10.1007/s13202-022-01533-x>.
- Aydin, A. (2013). Upgraded ISRM Suggested Method for Determining Sound Velocity by Ultrasonic Pulse Transmission Technique. *Rock Mechanics and Rock Engineering*, 47(1), 255–259. <https://doi.org/10.1007/s00603-013-0454-z>
- Agresti, A., & Finlay, B. (2018). *Statistical Methods for the Social Sciences*, Global Edition. Statistical Methods for the Social Sciences | Pearson library.
- Annual Financial Commitments in Renewable Energy. (2023). International Energy Agency IREA. <https://www.irena.org/Energy-Transition/Technology/Geothermal-energy>.
- Barbier, E. (2002). Geothermal energy technology and status: an overview. *Renewable and Sustainable Energy Reviews*, 6(1–2), 3–65. [https://doi.org/10.1016/s1364-0321\(02\)00002-3](https://doi.org/10.1016/s1364-0321(02)00002-3).
- Buryakovsky, L., Chilingar, G. V., Rieke, H. H., & Shin, S. (2012). *Petrophysics*. <https://doi.org/10.1002/9781118472750>.
- Bertini, G., Cappetti, G., & Fiordelisi, A. (2005). Geological features of Larderello-Travale and Mt. Amiata geothermal fields. *Geothermal Energy*, 2(1), 3-18. <https://doi.org/10.1186/s40517-022-00231-5>.
- Bischoff, A., Heap, M. J., Mikkola, P., Kuva, J., Reuschlé, T., Jolis, E. M., Engström, J., Reijonen, H., & Leskelä, T. (2024). Hydrothermally altered Shear zones: A new reservoir play for the expansion of deep geothermal exploration in crystalline settings. *Geothermics*, 118, 102895. <https://doi.org/10.1016/j.geothermics.2023.102895>.
- Bischoff, A., 1,2, Carbajal-Martinez, D., 2, Heap, M., 3, Reuschlé, T., 3, Kuva, J., 2, Jolis, E. M., 2, Cutts, K., 2, Kaiu Piipponen, University of Turku, Finland, Geological Survey of Finland, & University of Strasbourg, France. (2025). Crystal Clear: a petrophysical databank of crystalline rocks for assessing deep geothermal reservoirs in fault zones. https://media.voog.com/0000/0050/7355/files/EGC%202025_Bischoff_Crystal_Clear.pdf.

Bruhn, R.L., W.T. Parry, W. A Yonkee, and T. Thompson, Fracturing and hydrothermal alteration in normal fault zones, *Pageoph*, 142, 609-644, 1994.

Caspari, E., Greenwood, A., Baron, L., Egli, D., Toschini, E., Hu, K., & Holliger, K. (2020). Characteristics of a fracture network surrounding a hydrothermally altered Shear zone from geophysical borehole logs. *Solid Earth*, 11(3), 829–854. <https://doi.org/10.5194/se-11-829-2020>.

Cascade Institute. (2024, September 18). Drilling for Superhot Geothermal Energy: A Technology Gap Analysis - Cascade Institute. <https://cascadeinstitute.org/technical-paper/drillingreport/>.

Clauser, C., & Huenges, E. (2011). Thermal conductivity of rocks and minerals. In *AGU reference shelf* (pp. 105–126). <https://doi.org/10.1029/rf003p0105>.

Clauser, C., & Huenges, E. (1995). *Thermal conductivity of rocks and minerals*. In T. J. Ahrens (Ed.), *Rock Physics and Phase Relations: A Handbook of Physical Constants* (pp. 105–126). American Geophysical Union.

Chen, G. (2014). Steady-state heat transport: Ballistic-to-diffusive with Fourier's law. *Journal of Heat Transfer*, 136(9), 091302. <https://doi.org/10.1115/1.4027583>.

Deep Heat Flows (2024). Deep-HEAT-Flows Discovering Deep Geothermal Resources in Low-enthalpy Crystalline Settings. <https://deep-heat-flows.voog.com/>

Data Tab.. (2024). <https://datatab.net/tutorial/get-started>.

Energiateollisuus ry. (2023). District Heating in Finland 2023. In *Kaukolämpö*. https://energia.fi/wpcontent/uploads/2024/05/District_heating_in_Finland_2023.pdf.

Fossen, H., & Cavalcante, G. C. G. (2017). Shear zones – A review. In *Earth-Science Reviews*, Earth-Science Reviews [Journal-article]. <https://doi.org/10.1016/j.earscirev.2017.05.002>.

Frey, M., Bär, K., Stober, I., Reinecker, J., Van Der Vaart, J., & Sass, I. (2022). Assessment of deep geothermal research and development in the Upper Rhine Graben. *Geothermal Energy*, 10(1). <https://doi.org/10.1186/s40517-022-00226-2>.

Farndale, H., Law, R., & Geothermal Engineering Ltd. (2022). An update on the United Downs Geothermal Power Project, Cornwall, UK. In *Proceedings*, 47th

Workshop on Geothermal Reservoir Engineering: Vol. SGP-TR-223 (p. 1) [Journal-article].

Finsterle, S., Zhang, Y., Pan, L., Dobson, P., & Oglesby, K. (2013). Microhole arrays for improved heat mining from enhanced geothermal systems. *Geothermics*, 47, 104–115. <https://doi.org/10.1016/j.geothermics.2013.03.001>.

Flow, C. O. F. C. a. F., Resources, C. O. G. E. A., Studies, D. O. E. a. L., & Council, N. R. (1996). *Rock fractures and fluid flow: Contemporary Understanding and Applications*. National Academies Press.

Geothermal Energy. (2022). International Renewable Energy Agency IREA. <https://www.irena.org/Energy-Transition/Technology/Geothermal-energy>.

Geothermal Power Database. (2015). International Geothermal Association. <https://www.lovegeothermal.org/explore/our-databases/geothermal-power-database/>.

GTK 2022. Unpublished numerical models based on the Deep Geothermal Energy Potential Maps of Finland. https://hakku.gtk.fi/en/locations/search?location_id=194.

Gegenhuber, N., Schön, J., 2012. New approaches for the relationship between compressional wave velocity and thermal conductivity. *J. Appl. Geophysics*. 76:50–55. <http://dx.doi.org/10.1016/j.jappgeo.2011.10.005>.

Heap, M. J., Wadsworth, F. B., & Jessop, D. E. (2023). The Thermal conductivity of unlithified granular volcanic materials: The influence of hydrothermal alteration and degree of water saturation. *Journal of Volcanology and Geothermal Research*, 435, 107775. <https://doi.org/10.1016/j.jvolgeores.2023.107775>.

Hartmann, A., Rath, V., & Clauser, C. (2005). Thermal conductivity from core and well log data. *International Journal of Rock Mechanics and Mining Sciences*, 42(7–8), 1042–1055. <https://doi.org/10.1016/j.ijrmms.2005.05.015>.

Han, D., 1986. Effects of Porosity and Clay Content on Acoustic Properties of Sandstones and Unconsolidated Sediments, PhD dissertation, Stanford University, CA, 219 pp. Effects of porosity and clay content on acoustic properties of sandstones and unconsolidated sediments.

Haneberg, W. C. (1999). *Faults and subsurface fluid flow in the shallow crust*. American Geophysical Union.

Hadley, C. (2011). *Phonon transport and the Boltzmann transport equation*. TUWien. https://lampz.tugraz.at/~hadley/ss2/transport/phonon_Boltzmann.php

Inskip, N. F., Harpers, N., Shail, R., Claes, H., Hartog, S. D., & Busch, A. (2023). Reservoir properties of fault-related hydrothermally altered granites in Cornwall: Implications for geothermal energy prospectivity. Authored. <https://doi.org/10.22541/essoar.170110671.11387934/v1>.

Igel, H. (n.d.). *Seismology and the Earth's deep interior*. In *Elasticity and Seismic Waves*. Retrieved March 22, 2025, from https://www.geophysik.uni-muenchen.de/~igel/Lectures/Sedi/sedi_elastic.pdf

Jolie, E., Scott, S., Faulds, J., Chambert, I., Axelsson, G., Gutiérrez-Negrín, L. C., Regensburg, S., Ziegler, M., Ayling, B., Richter, A., & Zemedkun, M. T. (2021). Geological controls on geothermal resources for power generation. *Nature Reviews Earth & Environment*, 2(5), 324–339. <https://doi.org/10.1038/s43017-021-00154-y>.

Kukkonen, I. T. & Geological Survey of Finland. (1999). GEOTHERMAL ENERGY IN FINLAND. In the Geological Survey of Finland. <https://www.geothermalenergy.org/pdf/IGAstandard/WGC/2000/R0778.PDF>.

Kearey, P., Brooks, M., & Hill, I. (2013b). *An Introduction to Geophysical Exploration*. John Wiley & Sons.

Kukkonen, I., & Peltoniemi, S. (1998). Relationships between thermal and other petrophysical properties of rocks in Finland. *Physics and Chemistry of the Earth*, 23(3), 341–349. [https://doi.org/10.1016/s0079-1946\(98\)00035-4](https://doi.org/10.1016/s0079-1946(98)00035-4).

Kukkonen, I. T., Heikkinen, P. J., Malin, P. E., Renner, J., Dresen, G., Karjalainen, A., Rytönen, J., & Solantie, J. (2023). Hydraulic conductivity of the crystalline crust: Insights from hydraulic stimulation and induced seismicity of an enhanced geothermal system pilot reservoir at 6 km depth, Espoo, southern Finland. *Geothermic*, 112, 102743. <https://doi.org/10.1016/j.geothermics.2023.102743>.

Kukkonen, I. T., & Pentti, M. (2021). St1 Deep Heat Project: Geothermal energy to the district heating network in Espoo. *IOP Conference Series Earth and Environmental Science*, 703(1), 012035. <https://doi.org/10.1088/1755-1315/703/1/012035>.

Kittel, C. (2004). *Introduction to Solid State Physics*. Wiley.

Kim, H., Cho, J., Song, I., & Min, K. (2012). Anisotropy of elastic moduli, P-wave velocities, and thermal conductivities of Asan Gneiss, Boryeong Shale, and Yeoncheon Schist in Korea. *Engineering Geology*, 147–148, 68–77. <https://doi.org/10.1016/j.enggeo.2012.07.015>.

Letelier, J. A., O'Sullivan, J., Reich, M., Veloso, E., Sánchez-Alfaro, P., Aravena, D., Muñoz, M., & Morata, D. (2020). Reservoir architecture model and heat transfer modes in the El Tatio-La Torta geothermal system, Central Andes of northern Chile. *Geothermics*, 89, 101940. <https://doi.org/10.1016/j.geothermics.2020.101940>.

Ledésert, B., Hebert, R., Genter, A., Bartier, D., Clauer, N., & Grall, C. (2009). Fractures, hydrothermal alterations, and permeability in the Soultz Enhanced Geothermal System. *Comptes Rendus Géoscience*, 342(7–8), 607–615. <https://doi.org/10.1016/j.crte.2009.09.011>.

Mielke, P., Bär, K., & Sass, I. (2017). Determining the relationship between Thermal conductivity and compressional wave velocity of common rock types as a basis for reservoir characterization. *Journal of Applied Geophysics*, 140, 135–144. <https://doi.org/10.1016/j.jappgeo.2017.04.002>.

Motra, H. B., & Stutz, H. H. (2018). Geomechanical rock properties using pressure and temperature dependence of elastic P- and S-Wave velocities. *Geotechnical and Geological Engineering*, 36(6), 3751–3766. <https://doi.org/10.1007/s10706-018-0569-9>.

Martin. (2023, October 19). Energy - United Nations Sustainable Development. United Nations Sustainable Development. <https://www.un.org/sustainabledevelopment/energy/>.

Nevada's Project Red unlocks new potential for geothermal energy | Caliber. Az. (2024, December 18). Caliber.az. <https://caliber.az/en/post/nevada-s-project-red-unlocks-new-potential-for-geothermal-energy>.

Özkahraman, H.T., Selver, R., Işık, E.C., 2004. Determination of the Thermal conductivity of rock from P-wave velocity. *Int. J. Rock Mech. Min. Sci.* 41 (4):703–708. <http://dx.doi.org/10.1016/j.ijrmms.2004.01.002>.

OpenStax. (2016). *University Physics Volume 1*. OpenStax. <https://openstax.org/books/university-physics-volume-1>

PetroWiki. (2024b, March 31). Porosity determination with NMR logging - PetroWiki.

PetroWiki. (2024a, March 31). *Porosity determination with NMR logging* - PetroWiki. https://petrowiki.spe.org/Porosity_determination_with_NMR_logging.

Popov, Y., Tertychnyi, V., Romushkevich, R., Korobkov, D., & Pohl, J. (2003). Interrelations Between Thermal Conductivity and Other Physical Properties of Rocks: Experimental Data. *Pure and Applied Geophysics*, 160(5–6), 1137–1161. <https://doi.org/10.1007/pl00012565>.

Perkowitz, & Sidney. (2025, March 10). *Phonon | Quantum Mechanics, Wave-Particle Duality & Thermal Properties*. Encyclopaedia Britannica. <https://www.britannica.com/science/phonon>.

Riazi, N., Clarkson, C., Ghanizadeh, A., Vahedian, A., Aquino, S., & Wood, J. (2017). Determination of elastic properties of tight rocks from ultrasonic measurements: Examples from the Montney Formation (Alberta, Canada). *Fuel*, 196, 442–457. <https://doi.org/10.1016/j.fuel.2017.01.084>.

Schön, J. (2011). *Physical Properties of Rocks: A Workbook*. Elsevier.

Sustainable Energy for All. (2024, August 30). *Sustainable Energy for All Annual Report 2023*. https://www.seforall.org/system/files/2024-08/SEforALL-annual-report_2023_web-version.pdf.

Starzec, P. & Chalmers University of Technology. (1999). Dynamic elastic properties of crystalline rocks from south-west Sweden. In *International Journal of Rock Mechanics and Mining Sciences* (Vol. 36, pp. 265–272). [https://doi.org/10.1016/S0148-9062\(99\)00011-X](https://doi.org/10.1016/S0148-9062(99)00011-X).

Stawikowski, W. (2017). *Structural Geology* (2nd edition). *Geologos*, 23(2), 139–140. <https://doi.org/10.1515/logos-2017-0016>.

Schumann, K., Stipp, M., Behrmann, J. H., Klaeschen, D., & Schulte-Kortnack, D. (2014). PandSwave velocity measurements of water-rich sediments from the Nankai Trough, Japan. *Journal of Geophysical Research Solid Earth*, 119(2), 787–805. <https://doi.org/10.1002/2013jb010290>.

Shearer, P. M. (2019). *Introduction to seismology*. Cambridge University Press.

Tiab, D., & Donaldson, E. C. (2012). *Petrophysics: Theory and Practice of Measuring Reservoir Rock and Fluid Transport Properties*. Gulf Professional Publishing.

Vosteen, H., & Schellschmidt, R. (2003). Influence of temperature on thermal conductivity, thermal capacity and thermal diffusivity for different types of rock. *Physics and Chemistry of the Earth Parts a/B/C*, 28(9–11), 499–509. [https://doi.org/10.1016/s1474-7065\(03\)00069-x](https://doi.org/10.1016/s1474-7065(03)00069-x)

Weydt, L. M., Lucci, F., Lacinska, A., Scheuven, D., Carrasco-Núñez, G., Giordano, G., Rochelle, C. A., Schmidt, S., Bär, K., & Sass, I. (2022). The impact of hydrothermal alteration on the physiochemical characteristics of reservoir rocks: the case of the Los Humeros geothermal field (Mexico). *Geothermal Energy*, 10(1). <https://doi.org/10.1186/s40517-022-00231-5>.

Wang, Q., Ji, S., Sun, S., & Marcotte, D. (2009). Correlations between compressional and Shear wave velocities and corresponding Poisson's ratios for some common rocks and sulfide ores. *Tectonophysics*, 469(1–4), 61–72. <https://doi.org/10.1016/j.tecto.2009.01.025>.

Wyering, L., Villeneuve, M., Wallis, I., Siratovich, P., Kennedy, B., Gravley, D., & Can't, J. (2014). Mechanical and physical properties of hydrothermally altered rocks, Taupo Volcanic Zone, New Zealand. *Journal of Volcanology and Geothermal Research*, 288, 76–93. <https://doi.org/10.1016/j.jvolgeores.2014.10.008>.

Williams, C.F., Anderson, R.N., 1990. Thermophysical properties of the Earth's crust: in situ measurements from continental and ocean drilling. *J. Geophysics. Res. Solid Earth* 95 (B6):9209–9236. <http://dx.doi.org/10.1029/JB095iB06p09209>.

Weydt, L. M., Lucci, F., Lacinska, A., Scheuven, D., Carrasco-Núñez, G., Giordano, G., Rochelle, C. A., Schmidt, S., Bär, K., & Sass, I. (2022). The impact of hydrothermal alteration on the physiochemical characteristics of reservoir rocks: the case of the Los Humeros geothermal field (Mexico). *Geothermal Energy*, 10(1). <https://doi.org/10.1186/s40517-022-00231-5>.

Wikipedia contributors. (2024, July 23). *Heat transfer physics*. Wikipedia. https://en.wikipedia.org/wiki/Heat_transfer_physics.

Yu, C., Ji, S., & Li, Q. (2015). Effects of porosity on seismic velocities, elastic moduli and Poisson's ratios of solid materials and rocks. *Journal of Rock Mechanics and Geotechnical Engineering*.

Zhao, G., Ding, W., Tian, J., Liu, J., Gu, Y., Shi, S., Wang, R., & Sun, N. (2021). Spearman rank correlations analysis of the elemental, mineral concentrations, and mechanical parameters of the Lower Cambrian Niutitang shale: A case study in the Fenggang block, Northeast Guizhou Province, South China. *Journal of Petroleum Science and Engineering*, 208, 109550. <https://doi.org/10.1016/j.petrol.2021.109550>.

Ziman, J. M. (1960). *Electrons and Phonons: The Theory of Transport Phenomena in Solids*. Oxford University Press.

APPENDIX A

Codes used for Statistical Analysis- Example Thermal conductivity vs P-wave velocity can be reached out by using this link

<https://github.com/Wasim2112/Python-codes-for-analysis>.

Data used for this study

[Deep-HEAT-Flows_Petrophysics_delivery_20241126.xlsx](#)

APPENDIX B

Table 1: Results of statistical tests examining the association between P-wave velocity and porosity.

Porosity (%)	0-3 %	3-6 %	6-9 %	Above 9 %	Combined
Spearman's r value	-0.662	-0.011	-0.05	-0.400	-0.813
Statistical value (t_s) (Spearman)	-7.74	-0.04	-0.15	-0.617	-14.35
Critical value (t_c)	1.99	2.16	2.31	4.30	1.98
Chi-square p value	0	0.13	0.715	1.00	0
Chi-square statistics	30.25	7.1	2.11	0	52.67
Critical Value	9.48	9.48	9.48	3.84	9.48
Fisher exact value	0	0.619	1	1	0

Table 2: Results of statistical tests for S-wave velocity versus porosity.

Porosity (%)	0-3 %	3-6 %	6-9 %	Above 9 %	Combined
Spearman's r value	-0.313	-0.19	-0.34	-0.4	-0.61
Statistical value (Spearman)	-2.89	-0.7	-1.04	-0.62	-8.0
Critical value (Spearman)	1.99	2.2	2.3	4.3	1.98
Chi-square p value	0.14	0.062	0.8	1	0
Statistical value (Chi square)	6.9	8.98	1.7	0	41.1
Critical Value (Chi square)	9.48	9.48	9.48		9.48
Fisher exact value	0.37	1	1	1	0.00

Table 3: Results of statistical tests for compressional wave velocity versus density.

Porosity (%)	0-3 %	3-6 %	6-9 %	Above 9 %	Combined
Spearman's r value	0.294	0.172	0.212	0.8	0.565
Statistical value (Spearman)	2.69	0.63	0.613	1.88	7.04
Critical value (Spearman)	1.99	2.16	2.30	4.3	1.98
Chi-square p value	0.184	0.011	0.108	1	0
Statistical value (Chi square)	6.211	13	4.44	0	39.4
Critical Value (Chi square)	9.48	9.48	5.99	3.84	9.48
Fisher exact value	0.82	0.31	1	0.33	0.00009

Table 4: Results of statistical analysis for S-wave velocity versus density.

Porosity (%)	0-3 %	3-6 %	6-9 %	Above 9 %	Combined
Spearman's r value	0.3	0.01	0.2	0.8	0.51
Statistical value (Spearman)	2.78	0.04	0.6	1.88	6.11
Critical value (Spearman)	1.99	2.16	2.3	4.3	1.98
Chi-square p value	0.016	0.084	0.794	1	0
Statistical value (Chi square)	12.1	8.20	1.680	0	26.6
Critical Value (Chi square)	9.48	9.48	9.48	3.84	9.48
Fisher exact value	0.11	0.619	1.0	0.33	0.08

Table 5: Results of statistical analysis for acoustic impedance versus porosity.

Porosity (%)	0-3 %	3-6 %	6-9 %	Above 9 %	Combined

Spearman's r value	-0.67	-0.15	-0.08	-0.4	-0.83
Statistical value (Spearman)	-7.83	-0.53	-0.22	-0.62	-15.1
Critical value (Spearman)	1.99	2.16	2.31	4.3	1.98
Chi-square p value	0.001	0.498	0.28	1	0
Statistical value (Chi square)	18.48	3.37	5.1	0	63
Critical Value (Chi square)	9.48	9.48	9.48	3.84	9.48
Fisher exact value	0	1	1	1	0

Table 6: Results of statistical analysis for shear impedance versus porosity.

Porosity (%)	0-3 %	3-6 %	6-9 %	Above 9 %	Combined
Spearman's r value	-0.38	-0.25	-0.33	-0.4	-0.67
Statistical value (Spearman)	-3.58	-0.93	-0.99	-0.617	-9.1
Critical value (Spearman)	1.99	2.16	2.3	4.3	1.98
Chi-square p value	0.005	0.32	0.58	1.00	0
Statistical value (Chi square)	15	4.66	2.89	0.00	49.5
Critical Value (Chi square)	9.48	9.48	9.48		9.48
Fisher exact value	0.37	1	1	1	0

Table 7: Equations, type of fitting, and R² values for the response and explanatory variables.

Parameter 1	Parameter 2	Equation/Relationship	Fitting type	R²
P	ρ	$P = (4.9019) \rho - 7351$	Linear	0.61
S	ρ	$S = (2.7658) \rho - 4214.3$	Linear	0.4

S	φ	$S = -(113.71) \varphi + 3244.5$	Linear	0.5
AI	λ	$AI = (2.0183) \lambda + 7.5455$	Linear	0.22
SI	λ	$SI = (1.5915) \lambda + 2.3123$	Linear	0.19
SI	φ	$SI = (-0.4267) \varphi + 8,3736$	Linear	0.5

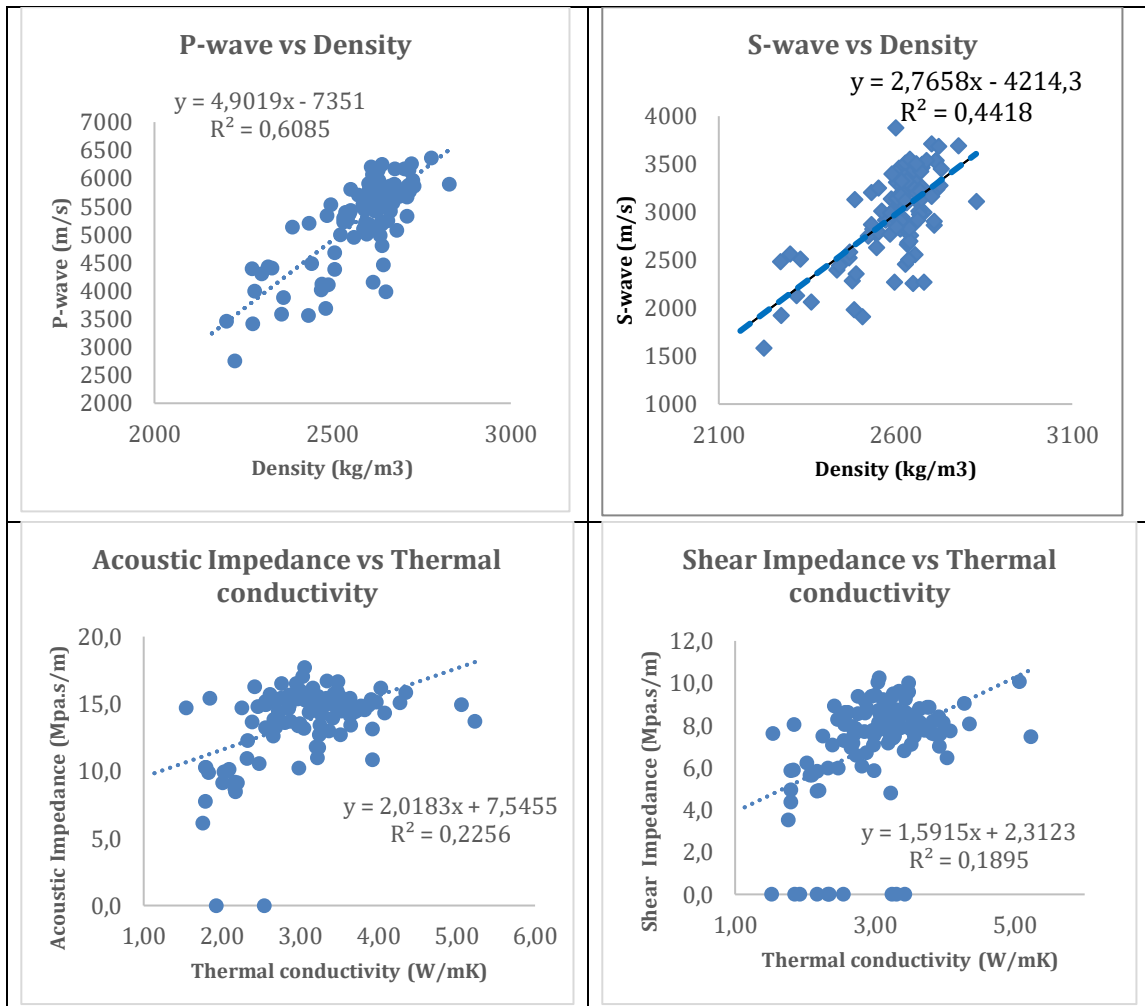


Figure 1: Regression analysis of seismic wave velocities, seismic impedances, density, and thermal conductivity. *Source: Produced with Microsoft Excel.*